PHYSICAL REVIEW C VOLUME 39, NUMBER 4 APRIL 1989

Toward a quantum chromodynamical derivation of nuclear physics

Gerald A. Miller
Institute for Nuclear Theory, Department of Physics, FM-15, University of Washington, Seattle, Washington 98195
(Received 4 October 1988)

The connection between the strong-coupling approximation to quantum chromodynamics and nuclear properties observed at low and medium energies and momentum transfer is examined. The strong-coupling approximation to quantum chromodynamics indicates that, for nuclei, the Pauli principle is obeyed at the hadronic level, so that quarks in different hadrons are treated as distinguishable objects. Furthermore, the gluonic effects of flux-tube rearrangement are small. Instead, a more significant strong-coupling approximation to quantum chromodynamics string-breaking term leads to meson emission from baryons. This mechanism is used to compute meson-nucleon and delta coupling constants and form factors. Qualitative agreement with experiment is achieved. Thus the strong-coupling approximation to quantum chromodynamics reproduces the salient features of the meson-baryon picture of low momentum transfer nuclear physics.

I. INTRODUCTION

Baryons and mesons are the building blocks of ordinary nuclei. However, quantum chromodynamics (QCD), with its quarks and gluons, is widely regarded to be the fundamental theory of the strong interaction. Therefore I ask if QCD can reproduce the baryon-meson dynamics of ordinary nuclei.

The purpose of such a question is two-fold. First, one can attempt to use the existence of nuclei to test the validity of QCD. Secondly, any derivation of baryonic aspects of conventional nuclear physics is expected to be approximate, and to break down at sufficiently high momentum transfer. Studying the breakdown may indicate the experiments to search for the onset of true quark and gluon degrees of freedom in nuclei. The present paper is intended as a first effort in applying QCD to understand the nucleus; only qualitative aspects are discussed.

One way to address such questions would be to employ lattice simulations, but current computer technology is not in a sufficiently advanced stage. Instead, one may use and model the strong coupling lattice QCD (SCQCD) Hamiltonian.[1-4] The name SCQCD arises as follows. The lattice spacing, a, (if large enough) provides a momentum scale for which the strong coupling constant, g, takes on large values. Thus one is able to treat the Hamiltonian by making low-order perturbation expansions in terms of inverse powers of g. The use of this expansion involves a departure from QCD, because, in general, one is not able to take the continuum limit of a (hence g) approaching zero. However, long-range phenomena are of most relevance to nuclear physics, so the strong-coupling expansion may be suitable.

I repeat: The basic assumptions of this work are that the strong coupling limit correctly describes the necessary features of the long distance behavior of QCD, and that one need not take to the continuum limit ($g^2 \to 0$) in order to understand the low momentum transfer physics of the continuum theory. Thus, SCQCD, as defined previously, is *not* QCD. A conclusion drawn correctly from SCQCD may turn out to be invalid. Nevertheless, it is interesting to examine the implications of SCQCD for nuclear physics. This has not been done. Furthermore, one should recall that SCQCD was the first technique to yield the long-range linear confining potential. This result survived the necessary more detailed lattice simulations. Indeed, strong coupling calculations of the string tension can be carried out sufficiently so that a smooth joining to the weak coupling region (scaling) is obtained.[5]

Using SCQCD to compute the entire nuclear wave function is not necessary. One derives the conventional description of nuclei by starting with a two-nucleon interaction and subjecting the nucleons to the Pauli principle.[6] Thus, it is reasonable to study the Pauli principle of composite nucleons, and examine the connection between SCQCD and the nucleon-nucleon interaction. There are some striking qualitative questions which require answers. What are the main features implied by SCQCD? Does SCQCD predict elements or terms entirely different from the conventional meson-exchange picture? Does SCQCD predict three and higher body interactions very different from what is now expected? The goal of this paper is to address these issues.

The results are that for nuclei, SCQCD indicates that quarks in different hadrons may be treated as distinguishable. (This may be necessary for the very existence of the nuclear shell model.[7]) It is also shown that SCQCD leads naturally to the idea that nucleons interact by meson exchange. Moreover, the values of pion-nucleon and omega-nucleon coupling constants computed in the framework of SCQCD are qualitatively consistent with observations. Thus, SCQCD seems to yield the conventional baryon-meson picture of nuclei at low and intermediate energies.

Here is an outline of the paper. In Sec. II, the lattice-regulated, locally-gauge invariant Hamiltonian is discussed. The ideas of strong coupling QCD have been used to develop phenomenological wave functions of the

mesons and baryons.[8–11] The phenomenologies and the theory are related in Sec. III. Furthermore, I show how to use continuum wave functions to evaluate matrix elements of the lattice Hamiltonian. In Sec. IV the requirements of local gauge invariance are shown to lead to the result that the baryonic Pauli principle applies in nuclei.

Another set of terms occur when the magnetic field energy leads to gluonic interactions called flux-tube rearrangements. Such effects are potentially very different from those of meson exchanges, but seem very small[12] as discussed in Sec. V. Then the dominant interaction between hadrons would arise through breaking of the color-flux tubes. Local gauge invariance requires that such flux-tube or string-breaking effects lead to quark-pair formation.

Quark-pair formation can lead to meson emission. Approximate treatments of the string-breaking part of the SCQCD Hamiltonian[13,14] are discussed, and the meson-baryon coupling constants are computed in Sec. VI. A final section is reserved for summary remarks and discussion of possible improvements, extensions, and implications.

II. THE SCQCD HAMILTONIAN

The Hamiltonian formulation of QCD is to be applied towards understanding nuclear physics. This treatment has been reviewed extensively,[1–4,15] so only features of relevance to the following applications are reproduced.

The Hamiltonian of QCD is amenable to an approximate treatment[1–4] in which three-dimensional space is treated as a discrete lattice of points. The time variable remains continuous. The points on the lattice are denoted by the vector $\mathbf{x}$. The links l join the points $\mathbf{x}$ and $\mathbf{x}+a\hat{\mathbf{e}}$ and where a is the lattice spacing and $\hat{\mathbf{e}}$ is one of six unit vectors: up, down, left, right, forward and back. The lattice theory is constructed so that the correct continuum limit (a goes to 0) and local gauge invariance (LGI) are maintained. LGI is needed to satisfy the requirement that every point in space be color neutral.

I next describe the lattice variables, beginning with the color electric field. As in the continuum theory, the electric field is the momentum variable canonically conjugate to the vector potential. Thus the electric field is the time derivative of the vector potential $\mathbf{A}$ [a three by three color SU(3) matrix], and the temporal gauge ($A_0=0$) is used. The lattice version of the electric field is $E(l)$ where the electric field lies on the link l (between $\mathbf{x}$ and $\mathbf{x}+a\hat{\mathbf{e}}$) and is parallel to the vector $\hat{\mathbf{e}}$. The electric contribution of the energy, H_E, can be written as[1]

$$H_E=\frac{g^2}{2a}\sum_l E(l)\cdot E(l)\ , \tag{2.1}$$

which is the lattice version of the familiar term involving the volume integral of E^2. The proportionality to g^2 results from a convenient definition of electric units.[1]

The lattice equivalent of the vector potential $\mathbf{A}$ is the operator $U(\mathbf{x},\hat{\mathbf{e}})[=U(l)]$

$$U(\mathbf{x},\hat{\mathbf{e}})=P\exp\left[i\int_{\mathbf{x}}^{\mathbf{x}+a\hat{\mathbf{e}}}\mathbf{A}(\mathbf{z})\cdot d\mathbf{z}\right]\ . \tag{2.2}$$

The local gauge transformation (LGT)

$$\begin{aligned} &q(\mathbf{x})\rightarrow S(\mathbf{x})q(\mathbf{x})\ ,\\ &U(\mathbf{x},\hat{\mathbf{e}})\rightarrow S(\mathbf{x}+a\hat{\mathbf{e}})U(\mathbf{x},\hat{\mathbf{e}})S^{-1}(\mathbf{x})\ , \end{aligned} \tag{2.3}$$

(where $S(\mathbf{x})$ is a unitary color matrix) reduces to the continuum form for small values of a. The term $q(x)$ is the quark field operator. The plaquette operator U_p,

$$U_p=\mathrm{Tr}U(1)U(2)U(3)U(4)\ , \tag{2.4}$$

[see Fig. 1(a)] is used to construct the magnetic field contribution to the Hamiltonian[1]

$$H_M=\frac{1}{ag^2}\sum_p(6-U_p-U_p^\dagger)\ . \tag{2.5}$$

The dynamics of the gauge boson field is specified by stating the lattice version of the canonical commutation relations

$$[E^\alpha(l),U_{ij}(l')]=\tfrac{1}{2}[\lambda^\alpha U(l)]_{ij}\delta_{ll'}\ . \tag{2.6}$$

The description of the Hamiltonian is completed by specifying the quark contribution[2] (for quarks of zero bare mass)

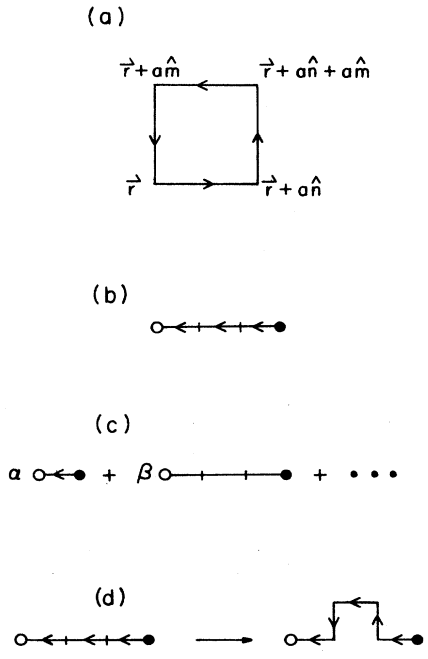

FIG. 1. Lattice dynamics. (a) A plaquette. (b) A gauge invariant $q\bar{q}$ pair, $n=3$. (c) Some (one-dimensional) components of a physical meson wave function. (d) An example of the action of H_M on the configuration of (b). In this and other figures, quarks are represented by filled circles, antiquarks by open circles, and flux lines by lines.

$$H_q=\frac{i}{2a}\sum_r\{[\chi^\dagger(r)U(r,\hat{\mathbf{n}}_z)\chi(r+\hat{\mathbf{n}}_z) -\chi^\dagger(r+\hat{\mathbf{n}}_z)U^{-1}(r,\hat{\mathbf{n}}_z)\chi(r)] \times(-1)^y+\text{cyc. perm.}\}\ , \tag{2.7}$$

in which "staggered" fermions are used, species doubling is eliminated and, chiral symmetry is maintained. The index r stands for (x,y,z). The field operators $\chi(\mathbf{r})$ are singlets in spin and isospin, come in three colors,[2] and have eight components representing the 4 (Dirac)×2 (isospin) components of the quark field operator, q. Strange and charmed quarks can also be included.

Adding up all the contributions, one finds the lattice Hamiltonian H

$$H=H_E+H_q+H_M\ . \tag{2.8}$$

The terms in this expression are written in the order g^n, with terms of highest power of n appearing first. The strong coupling expansion is defined by solving the theory of H_E exactly, and then treating the remaining terms as a perturbation. (The strong coupling expansion is not the favored method for lattice computations,[15] but I am interested in qualitative issues.) A modified strong coupling expansion is discussed in Sec. III.

The lattice version of the theory maintains the basic tenet that all states must be invariant under local gauge transformations. Physically, this is the statement that color vanishes at every lattice site. For example, the configuration

$$q^+(\mathbf{x}+a\hat{\mathbf{e}})U(l)q(\mathbf{x})|0\rangle$$

($|0\rangle$ is the unperturbed vacuum) is invariant under the transformation (2.3).

To understand the theory let's examine the dynamics. Consider first, confinement. The unperturbed vacuum $|0\rangle$ is defined so that

$$E^a(l)|0\rangle=0\ . \tag{2.9a}$$

$$\langle 0|U(l)|0\rangle=0\ . \tag{2.9b}$$

Note that Eq. (2.9b) is a property of the physical vacuum. One may use the commutation relation (2.6) to show

$$E^2(l)U(l)|0\rangle=\tfrac{4}{3}U(l)|0\rangle\ . \tag{2.10}$$

Thus we see that the string-bit operators U create electric flux and energy. (Similarly, $U^\dagger$ can destroy electric flux and energy.) Recalling H_E, we see that the electric energy gets a contribution of $(\frac{2}{3})g^2/a$ for each term $U(l)$ acting on the unperturbed vacuum. A quark antiquark pair, separated by a line of n links, has an electric energy of na times $(\frac{2}{3})g^2/a$.[2] But na is just the distance between the fermions, Fig. 1(b). Thus, one obtains the linear confining potential. (For strong coupling, g is proportional to a and the potential is independent of a.) This confinement is not spoiled by including higher order terms.[5] The basic result is that the operator H_E counts the number of flux links, it does not change that number.

Next, examine the quark Hamiltonian, H_q. This term causes both the quark kinetic energy and $q\bar{q}$ pair production (string breaking). H_q can destroy a quark, create a flux link, and create a quark. This can change the length of a $q\bar{q}$ pair joined by a flux line (a kinetic energy term) and also lead to the creation of a new $q\bar{q}$ pair (string-breaking or quark-pair creation).

The use of "staggered fermions" has interesting consequences. Quarks (antiquarks) exist only on even (odd) lattice sites. Therefore, mesons must consist of an odd number of links. The influence of this on the kinetic energy is that a mesonic component of length a can be converted to one of length $3a$ only by a two-step process in which the intermediate state has an extra "meson." Thus the imposition of the lattice version of chiral symmetry (2.7) leads to the close association of the quark kinetic energy operator (hence, constituent quark mass) with a cloud of mesons, and a contribution to the constituent quark mass is generated by a version of the Nambu Jona-Lasinio mechanism.[16]

This interesting feature is not exploited in this paper (see the following). In any case, the length of a string is not an eigenvalue so that a physical state is a superposition of strings of different lengths and shapes, Fig. 1(c).

The H_M term (B^2) is of order g^{-4} with respect to the E^2 term. It consists of plaquettes which destroy and create flux lines. Its action is to rearrange flux lines. See, for example, Fig. 1(c).

III. RELATING THE LATTICE HAMILTONIAN TO CONTINUUM HADRONIC WAVE FUNCTIONS

The previous section deals with the lattice Hamiltonian. In principle, one may use the strong coupling expansion to obtain energies and wave functions. However, the numerical difficulties are huge. Moreover, using continuum wave functions for the hadrons would increase the number of possible applications. In the following I indicate a general procedure to use continuum hadronic wave functions in the evaluation of the lattice Hamiltonian.

The Hamiltonian (2.8) may be rewritten as

$$H_{\text{QCD}}^{\text{SC}}=T+V+(H_q-T)+H_M+(H_E-V)\ , \tag{3.1}$$

in which T is a continuum fermion mass and kinetic energy term, and V is the usual linear potential σr between the quark and antiquark. The motivation for [3.1] is that one may define a solvable unperturbed Hamiltonian $H_0=T+V$ and, in principle, treat the remainder $H-H_0=H_1$ to all orders of perturbation theory. One can obtain the energy and wave functions of the Hamiltonian of Eq. (3.1) using standard perturbation theory.

The significance of Eq. (3.1) is that one can use continuum wave functions to evaluate matrix elements of the lattice Hamiltonian. As an example, consider the evaluation of H_E for a meson. Let $\phi_0(\mathbf{r})$ be the eigenfunction of H_0, where $\mathbf{r}$ is the $q\bar{q}$ separation. One may define a different lattice for each value of $\mathbf{r}$, and then divide r into n pieces of length a. Assuming that the electric flux line is parallel to r (see the following) each segment has an energy $\frac{2}{3}g^2/a\,(=\sigma a)$. Approximating the sum over line segments by an integral gives

$$\langle\phi|H_E|\phi\rangle=\sigma\int d^3r\, r|\phi(\mathbf{r})|^2\ . \tag{3.2}$$

Perturbative evaluations of Eq. (3.1) may define a reasonable strategy for a complete treatment. However, attaining such a goal is beyond present intentions. I only want to use (3.1) to understand the relationship between QCD and phenomenological applications.

With this in mind, examine the different contributions to H_1. Start with H_M. This term introduces kinks into the string and is responsible for the restoration of rotational symmetry and the roughening transition.[2,15] Furthermore, H_M causes the physical vacuum to acquire a gluon condensate. Calculations[17] show that the restoration of rotational symmetry occurs over a wider range in g^2 than one would expect.[18] For points that do not coincide with the axes of the lattice, a value of g^4 as small as two gives reasonably round equipotential surfaces. However, the situation is complicated. Kogut *et al.*[17] find that the restoration of rotational symmetry occurs in the weak coupling region of g. Merlin & Paton[19] obtain the restoration at a larger value of g ($g^4=4$) closer to the strong coupling region, indicating the adequacy of strong coupling theory. The flux tube can deviate from a straight line path. This wandering or "delocalization" leads to a contribution $-\pi/12r$ to the $q\bar{q}$ potential energy.[20]

Another problem is the thickness of the flux tube. Recent lattice calculations by Sommer[21] (who finds a narrow flux tube of diameter 0.2 fm), and Caldi and Sterling,[22] support the narrow flux tube picture. One may then imagine that the color electric flux is on the line between the quark and antiquark. However, long-wavelength oscillations of the flux line lead to a term $-\pi/12r$ which supplements the linear confining potential.

Consider next the term H_q-T. In the work of the Illinois[9] and Toronto[10,11] groups the continuum kinetic energy T is taken to be $(-\nabla^2+m^2)^{1/2}$. Corrections due to the finite-size lattice are not examined. In addition, the term H_q leads to emission of $q\bar{q}$ pairs, and therefore to hadronic decays via meson emission.[13,14] Such terms are discussed in Sec. VI. The magnetic spin dependent interactions also rise also from the H_q term.[23]

Putting all this together leads to the notion that strong coupling theory provides a reasonable qualitative approach. As long as $g\gtrsim 1.1$ ($a\gtrsim 0.11$ fm), the necessary higher-order corrections do not seem to destroy the basic picture of confinement and the need to use gauge invariant physical states. Thus one can attempt to apply SCQCD to nuclei by using flux line ideas. The first step is to recall significant features of phenomenological hadronic wave functions.

A. Phenomenological meson wave functions

The standard procedure for phenomenological applications is to supplement the confining term by the $-\pi/12r$ term, the color electric $1/r$ term, and the color-magnetic hyperfine interaction. For example, Carlson *et al.*,[9] and Godfrey and Isgur[10] have achieved an excellent description of mesonic spectra as well as various transition rates with this procedure. Kumano and Pandharipande[14] made the useful observation that using the hydrogen wave function

$$\psi_0(r)=2\nu^{3/2}e^{-\nu r}\ , \tag{3.3}$$

where $\nu=\sqrt{3}/(2R_M)$ and R_M is the rms radius of the meson M, is sufficient to reproduce matrix elements involving wave functions (of the same rms radius) determined from variational methods.

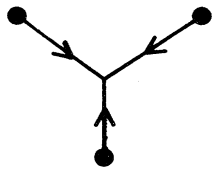

FIG. 2. Locally gauge-invariant flux-line configuration for a baryon.

B. Baryonic wave functions

The baryons are treated with a set of approximations that are similar to the ones made for mesons except for one essential difference. Local gauge invariance requires the electric field energy to be treated as a three-body potential: Writing the baryon state in a local gauge-invariant manner, along with assuming linear flux, leads to the geometry of Fig. 2. The introduction of a coordinate (R), additional to the three quark coordinates ($\mathbf{r}_1,\mathbf{r}_2,\mathbf{r}_3$), is necessary to preserve local gauge invariance. The total electric field energy is taken to be proportional to the sum of the lengths:

$$V=\sigma\sum_{i=1}^{3}|\mathbf{r}_i-\mathbf{R}|\ .$$

In this case the electric flux lies along each of the three vectors $\mathbf{r}_i-\mathbf{R}$. One determines $\mathbf{R}$ by minimizing V with respect to $\mathbf{R}$. Variational calculations determine the spectra and wave functions. Excellent reproductions of the data are achieved by Carlson *et al.* and Capstick and Isgur. However the preceding ansatz is not yet supported by lattice calculations.

One possible problem is the size of the baryons. For example, the computed radius of the nucleon is about 0.3 fm according to Carlson *et al.* and 0.4 fm in the Capstick-Isgur calculation. Meson cloud and recoil terms could increase the computed value of the nucleon size.

IV. LOCAL GAUGE INVARIANCE AND THE PAULI PRINCIPLE

The construction of nucleon wave functions in accord with the criteria of local gauge invariance (LGI) has important implications. Greenberg and Hieterinta[24,25] (GH) implemented LGI by introducing a link-operator formalism. GH showed that LGI leads to models in which quarks in different hadrons act as distinguishable objects. Inner products between two-hadron states have

only those terms expected for Bose mesons and Fermi baryons considered as elementary particles because overlap terms arising from contractions of quark operators in one baryon with quark operators in another vanish.

The intent of this section is to show that SCQCD leads to the GH result. I discuss the significance of this before giving the details.

Consider the motion of composite sizeable nucleons through the nucleus. If two such objects are close, a quark in one nucleon can be at the same position as a quark in another. If the quarks behave in the same manner as electrons in molecules, quark exchange effects, arising from the Pauli principle, are present.[26]

However significant, quantum electrodynamic (QE) effects lead to a breakdown of the nuclear shell model. Let's follow Krein and Maris[7] here. They start with Weisskopf's[27] derivation of the shell model. For nucleons in the medium the nucleon-nucleon interaction is the Bruckner G-matrix

$$G=\langle \mathbf{p}_1'\mathbf{p}_2'|QV|\psi_{\mathbf{p}_1\mathbf{p}_2}\rangle ,$$

in which $\mathbf{p}_i$ and $\mathbf{p}_i'$ are the initial and final momenta of individual nucleons, $\psi_{\mathbf{p}_1,\mathbf{p}_2}$ is the wave function, and where Q is a projection operator for nucleons above the Fermi sea. For $p_1,p_2<p_f$ energy-momentum conservation says $p_1',p_2'<p_f$, and therefore $\langle \mathbf{p}_1'\mathbf{p}_2'|Q=0$. Thus, G and the scattering cross section σ vanish, so the mean free path $\lambda(\lambda=1/\rho\sigma)$ is infinite. One obtains an independent particle shell model, even though V is quite large.

Krein & Maris reexamined the equation $\langle \mathbf{p}_1'\mathbf{p}_2'|Q=0$ using composite nucleons. The key point is that QE causes $\langle \mathbf{p}_1'\mathbf{p}_2'|\mathbf{p}_3\mathbf{p}_4\rangle$ to be nonzero even if $p_1',p_2'<p_f$ and $p_3,p_4>p_f$. Thus, λ acquires a finite value. The exact value is not an issue. A λ as large as 20 fm would be a severe problem since the imaginary part of the shell model potential would be real. In the independent pair approximation, λ must be infinite, so QE does not seem compatible with the existence of the nuclear shell model.

Is there any way to avoid the preceding result? One way is if nucleons are very small and/or nucleon-nucleon repulsive interactions separate the nucleus, so QE effects are negligible anyway. It might also be that there are holes in the Fermi sea. Two nucleons in the Fermi sea can scatter into these openings. Such effects are of fourth order in the hole-line expansion, and are far less significant.

Thus the validity of the shell model indicates how nonperturbative QCD works. Namely, QE effects are very small. It is therefore interesting to see if SCQCD reproduces the necessary suppression of QE effects.

I now return to calculational details. GH did not derive a detailed relationship between their formalism and QCD, but stated that the link operators are an "abbreviated description of the infinite number of degrees of freedom associated with the gluon." The lack of a direct relationship with QCD means that one does not know how compelling is the GH conclusion about the Pauli principle. In later work, Robson[28] derived a relationship between the link operators of GH and the string-bit operators of QCD.

In this section I argue that the central results of GH emerge from SCQCD. This requires the assumption that the strong-coupling expansion, in which the gluonic degrees of freedom are treated in terms of flux lines, be a reasonable approximation. Explicit link operators are not required to obtain the present result that quarks in different hadrons can be treated as distinguishable. Meson-nucleon vertex functions are also examined. A nucleon can emit a quark-antiquark pair bound together as a meson. It turns out that the quark in the meson is distinguishable from the three quarks in the proton. Thus, SCQCD and the conventional dynamics of nuclear physics have significant points in common.

As a first step, we examine inner products between two-meson states. We take the quarks to be on lattice sites, so the paths are connected by the lattice links. Gluonic correlations of the vacuum are neglected here, but examined in Sec. IV A. It is useful to present some simpler matrix elements.[29] The basic one is

$$\langle 0|U_{\alpha\beta}^{\dagger}(\mathbf{r},\hat{\mathbf{m}})U_{\gamma\delta}(\mathbf{r},\hat{\mathbf{n}})|0\rangle=\delta_{\mathbf{r},\mathbf{r}'}\delta_{\hat{\mathbf{m}},\hat{\mathbf{n}}}\tfrac{1}{3}\delta_{\alpha\delta}\delta_{\beta\gamma} . \quad (4.1)$$

Note that Kronecker δ functions appear as a result of treating space discretely. Two states formed by a single link operator acting on the vacuum have a nonzero overlap if, and only if, the starting, ending points, and direction of the string-bit operator are the same. Next consider other terms:

$$\langle 0|U_{\alpha\beta}^{\dagger}(\mathbf{r}'+a\hat{\mathbf{n}}',\hat{\mathbf{m}}')U_{\beta\rho}^{\dagger}(\mathbf{r}',\hat{\mathbf{n}}')U_{\mu\nu}(\mathbf{r},\hat{\mathbf{n}})U_{\nu\delta}(\mathbf{r}+a\hat{\mathbf{n}},\hat{\mathbf{m}})|0\rangle=\delta_{\mathbf{r},\mathbf{r}'}\delta_{\hat{\mathbf{n}}\hat{\mathbf{n}}'}\delta_{\hat{\mathbf{m}},\hat{\mathbf{m}}'}\tfrac{1}{9}\delta_{\rho\mu}\delta_{\nu\beta} , \quad (4.2a)$$

but

$$\langle 0|[U(\mathbf{r},\hat{\mathbf{n}})U(\mathbf{r}+a\hat{\mathbf{n}},\hat{\mathbf{m}})]^2|0\rangle=0 . \quad (4.2b)$$

The last relation follows from

$$U(\mathbf{r},\hat{\mathbf{n}})U(\mathbf{r}+a\hat{\mathbf{n}},\hat{\mathbf{m}})=U(\mathbf{r},\mathbf{r}+a\hat{\mathbf{n}}+a\hat{\mathbf{m}};c) ,$$

and the result that $[U(\mathbf{r},\mathbf{r}';c)]^2$ cannot transform as a color singlet. (The notation $U(\mathbf{r},\mathbf{r}';c)$ denotes a flux line, starting at $\mathbf{r}$ and ending at $\mathbf{r}'$, along a path denoted by c.) With (4.1) and (4.2) as examples, one can state a result involving more general operators, $U(\mathbf{x},\mathbf{y};c)$, which are built from a connected string of link operators. This is

$$\langle 0|U_{\alpha\beta}^{\dagger}(\mathbf{x}',\mathbf{y}';c')U_{\gamma\delta}(\mathbf{x},\mathbf{y};c)|0\rangle=\delta_{\mathbf{x},\mathbf{x}'}\delta_{\mathbf{y},\mathbf{y}'}\delta_{cc'}\tfrac{1}{3}\delta_{\alpha\delta}\delta_{\beta\gamma}\equiv\tfrac{1}{3}\delta_{cc'}\delta_{\alpha\delta}\delta_{\beta\gamma} . \quad (4.3)$$

[Including the starting ($\mathbf{x}$) and ending points ($\mathbf{y}$) in the definition of the path c simplifies the notation.] The meaning of (4.3) is that two different paths formed by string-bit operators are orthogonal. Examples are shown in Fig. 3. The results (4.1)–(4.3) are essential to the derivation of the desired inner products. These are the mathematical relations of the string-bit operators. We shall assume that these operators are relevant for physical continuum states. This is the essential approximation.

Next consider a single meson state. We impose the requirements of local gauge invariance and Gallilean invariance to write

$$|M(\mathbf{p})=\sum_{\mathbf{x},\mathbf{y},c}(a^3)^2\frac{e^{i\mathbf{p}\cdot(\mathbf{x}+\mathbf{y})/2}}{(2\pi)^{3/2}}\frac{\chi_c}{\sqrt{3}}(|\mathbf{x}-\mathbf{y}|)d^\dagger_\beta(\mathbf{y})\Gamma U_{\beta\alpha}(\mathbf{x},\mathbf{y},c)b^\dagger_\alpha(\mathbf{x})|0\rangle\ , \tag{4.4}$$

in which $b^\dagger(\mathbf{x})[d^\dagger(\mathbf{y})]$ are that part of $\psi(\mathbf{x})[\psi^\dagger(\mathbf{y})]$ that creates quarks (antiquarks) with standard anticommutation relations. The indices α,β refer to color indices. Other indices are not written. The operator Γ acts on the flavor-spin degrees of freedom so that the appropriate quantum numbers are obtained. A discrete version of the wave function, as expected from the lattice Hamiltonian, is given here.

The function $\chi_c(|\mathbf{x}-\mathbf{y}|)$ weights the various paths from $\mathbf{y}$ to $\mathbf{x}$ by numerical factors. The strong coupling expansion predicts that the most important path c is the straight line from $\mathbf{y}$ to $\mathbf{x}$. The amplitude for other paths is reduced by at least one power of g^2. The total momentum of the state (4.4) is $\mathbf{p}$.

The intent is to examine mesonic overlaps. The simplest is $\langle M(\mathbf{p}')|M(\mathbf{p})\rangle$. Eq. (4.3) may be used to obtain

$$\langle M(\mathbf{p}')|M(\mathbf{p})\rangle=\sum_{\mathbf{r},c}a^3|\chi_c(\mathbf{r})|^2\mathrm{Tr}(\Gamma^\dagger\Gamma)\sum_{\mathbf{R}}\frac{a^3}{(2\pi)^3}e^{i(\mathbf{p}-\mathbf{p}')\cdot\mathbf{R}}\ . \tag{4.5a}$$

Approximating the summations over $\mathbf{r}$, c, and $\mathbf{r}$ by integration gives

$$\langle M(\mathbf{p}')|M(\mathbf{p})\rangle\approx\delta(\mathbf{p}-\mathbf{p}')\sum_c\int|\chi_c(|\mathbf{z}|)|^2d^3z\,\mathrm{Tr}(\Gamma^\dagger\Gamma)=\delta(\mathbf{p}-\mathbf{p}')\ . \tag{4.5b}$$

Using the equality sign in the first step of Eq. (4.5b) amounts to neglecting terms of higher order in a. Such terms are already neglected in deriving the Hamiltonian.

Now consider two-meson states formed by a direct product of states of Eq. (4.4). The overlap function

$$\langle M(\mathbf{p}_1)M(\mathbf{p}_2)|M(\mathbf{p}_3)M(\mathbf{p}_4)\rangle\equiv\mathcal{O}_M$$

involves using Eq. (4.4) four times. Use the four sets of coordinates $\mathbf{x}_i,\mathbf{y}_i$ and the four path indices c_i with $i=1,4$. Then $\mathcal{O}_M$ is a sum of integrals of products $\mathcal{O}_G\mathcal{O}_Q$. The "gluonic" terms have an overlap $\mathcal{O}_G$ with

$$\mathcal{O}_G=\langle 0|U^\dagger(c_2)U^\dagger(c_1)U(c_3)U(c_4)|0\rangle\ , \tag{4.6}$$

in which the abbreviated notation $c_i\equiv(\mathbf{x}_i,\mathbf{y}_i;c_i)$ is used. The quark terms require an overlap $\mathcal{O}_Q$:

$$\begin{aligned}\mathcal{O}_Q&=\langle 0|b(\mathbf{x}_2)d(\mathbf{y}_2)b(\mathbf{x}_1)d(\mathbf{y}_1)d^\dagger(\mathbf{y}_3)b^\dagger(\mathbf{x}_3)d^\dagger(\mathbf{y}_4)b^\dagger(\mathbf{x}_4)|0\rangle\\&=[\delta(\mathbf{y}_1,\mathbf{y}_3)\delta(\mathbf{y}_2,\mathbf{y}_4)-\delta(\mathbf{y}_1,\mathbf{y}_4)\delta(\mathbf{y}_2,\mathbf{y}_3)][\delta(\mathbf{x}_1,\mathbf{x}_3)\delta(\mathbf{x}_2,\mathbf{x}_4)-\delta(\mathbf{x}_1,\mathbf{x}_4)\delta(\mathbf{x}_2,\mathbf{x}_3)]\ ,\end{aligned} \tag{4.7}$$

with color flavor-spin indices suppressed. The terms of positive sign of (4.7), see Fig. 4(a), yield contributions to $\mathcal{O}_M$ of the form

$$\langle M(p_1)|M(p_3)\rangle\langle M(p_2)|M(p_4)\rangle$$

or

$$\langle M(p_1)|M(p_4)\rangle\langle M(p_2)|M(p_3)\rangle\ .$$

These are the direct terms. The negative terms of (4.7) are those in which a quark or antiquark are interchanged, as shown for example in Fig. 4(b). Such terms are dubbed "quark exchange."

Equation (4.7) is standard. Its use under the assumption that $\mathcal{O}_G=1$, leads to a variety of so-called[27] "quark-exchange effects." However, the presence of $\mathcal{O}_G$ kills the quark-exchange effects. To see this, use (4.7) to integrate over $\mathbf{x}_3,\mathbf{x}_4,\mathbf{y}_3,\mathbf{y}_4$ in $\mathcal{O}_M$. Then

$$\begin{aligned}\mathcal{O}_M=\sum_{\substack{c_1c_2\\c_3c_4}}\int d^3x_1d^3x_2d^3y_1d^3y_2e^{-i\mathbf{p}_1\cdot(\mathbf{x}_1+\mathbf{y}_2)/2}e^{-i\mathbf{p}_2\cdot(\mathbf{x}_1+\mathbf{y}_2)/2}\chi^+_{c_1}(|\mathbf{x}_1-\mathbf{y}_1|)\chi^+_{c_2}(|\mathbf{x}_2-\mathbf{y}_2|)\mathcal{O}_G\\\times\{[\chi_{c_3}(|x_1-\mathbf{y}_1|)\chi_{c_4}(|\mathbf{x}_2-\mathbf{y}_2|)e^{i\mathbf{p}_3\cdot(\mathbf{x}_1+\mathbf{y}_1)/2}e^{i\mathbf{p}_4\cdot(\mathbf{x}_2+\mathbf{y}_2)/2}+(3\rightleftharpoons4)]\\-[\chi_{c_3}(|\mathbf{x}_2-\mathbf{y}_1|)\chi_{c_4}(|\mathbf{x}_1-\mathbf{y}_2|)e^{i\mathbf{p}_3\cdot(\mathbf{x}_2+\mathbf{y}_1)/2}e^{i\mathbf{p}_4\cdot(\mathbf{x}_1+\mathbf{y}_2)/2}+(3\rightleftharpoons4)]\}\ .\end{aligned} \tag{4.8}$$

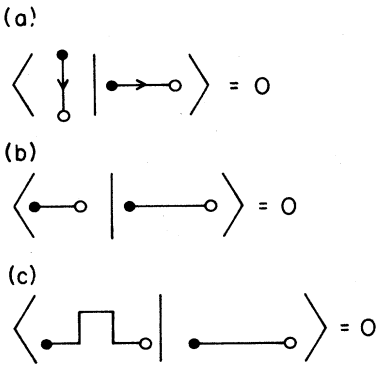

FIG. 3. Examples of orthogonal flux-line configurations leading to vanishing overlaps.

The factors Γ and $\sqrt{3}$ are omitted in (4.8) to simplify the notation. (Sums over $\mathbf{x}_i$ and $\mathbf{y}_i$ are approximated as integrals.) The first terms of the integral of (4.8) are the direct terms and the second are the exchange terms.

The overlap $\mathcal{O}_G$ is needed to evaluate Eq. (4.8). There are two cases of interest. First suppose the four curves c_i do not intersect. Then a direct evaluation using the ideas behind (4.1)–(4.3) yields

$$\mathcal{O}_G=[\delta(c_1,c_3)\delta(c_2,c_4)+\delta(c_1,c_4)\delta(c_2,c_3)] . \quad (4.9)$$

A simple example of Eq. (4.9) is given in Fig. 5(a). The use of (4.9) in (4.8) yields a contribution $[\mathcal{O}_M^{(0)}]$ to $\mathcal{O}_M$:

$$\mathcal{O}_M^{(0)}=\delta(\mathbf{p}_1-\mathbf{p}_3)\delta(\mathbf{p}_2-\mathbf{p}_4)+\delta(\mathbf{p}_1-\mathbf{p}_4)\delta(\mathbf{p}_2-\mathbf{p}_3) . \quad (4.10)$$

The result (4.10) follows from (4.5b) and the observation that the Kronecker δ functions of (4.9) cause the contributions of the exchange terms of (4.8) to be those of a set of measure zero. Thus the exchange terms vanish.

What happens if the curves do intersect? Then the result (4.9) is not obtained. Consider the initial state with all of the curves c_i straight lines. This is the relevant situation in the strong coupling limit. Drawing four straight lines, each beginning at a quark and ending on an antiquark, that have an infinite number of intersections is not possible. Thus the lowest energy configurations do not cause a correction of Eq. (4.10). Instead, one finds the situation of Fig. 5b, in which c_3 and c_4 are not straight lines. These correspond to higher than minimum energy components of the wave function. See Fig. 5c, in which the second term is smaller than the first by at least two powers of $1/g^2$. Hence, in the strong coupling limit terms of $\mathcal{O}_G$ with intersecting flux lines are of order $(1/g^2)^4$ and are negligible. Such effects are ignored.

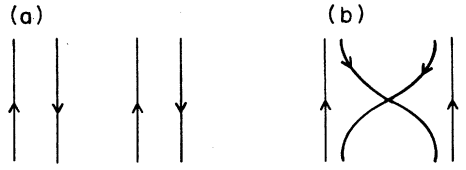

FIG. 4. Meson-meson overlaps; (a) a direct term, (b) an exchange term.

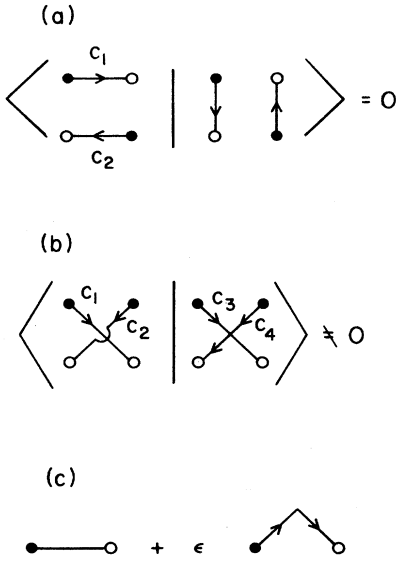

FIG. 5. Meson-meson overlaps with configurations obeying LGI.

The net result is that the meson-meson overlap function is

$$\langle M(\mathbf{p}_1)M(\mathbf{p}_2)|M(\mathbf{p}_3)M(\mathbf{p}_4)\rangle=\delta(\mathbf{p}_1-\mathbf{p}_3)\delta(\mathbf{p}_2-\mathbf{p}_4)+\delta(\mathbf{p}_1-\mathbf{p}_3)\delta(\mathbf{p}_2-\mathbf{p}_4) . \quad (4.11)$$

Equation (4.11) is the central one of this section. It requires the validity of the strong coupling expansion. This is that flux lines (as opposed to blobs) exist and that high-order ($n \geq 3$) terms in g^{-2n} are small.

A question of relevance to many-body physics is overlaps involving three (or more) meson states. The orthogonality properties of the U matrices, Eq. (4.3), lead to the result that matrix elements such as

$$\langle M(p_1)M(p_2)M(p_3)|M(p_4)M(p_5)M(p_6)\rangle$$

are simply those of the usual Bose mesons, again provided that the strong coupling expansion converges reasonably well.

Turn now to baryonic properties. I again argue that the gluonic overlaps kill the quark-exchange terms. Baryon wave functions are needed. Local gauge invariance leads to

$$|B\rangle=\sum_{\{c_i\}}\epsilon^{rst}\psi(\mathbf{x}_i,\mathbf{w},c_i)[U(\mathbf{w},\mathbf{x}_1,c_1)b^\dagger(\mathbf{x}_1)]^r \times[U(\mathbf{w},\mathbf{x}_2,c_2)b^\dagger(\mathbf{x}_2)]^s \times[U(\mathbf{w},\mathbf{x}_3,c_3)b^\dagger(\mathbf{x}_3)]^t|0\rangle\ . \tag{4.12}$$

Recall Fig. 2. The ϵ^{rst} is the usual totally antisymmetric tensor, invariant under LGT. Each of the terms in the sum of $\{c_i\}$ is invariant under the transformation (2.13). [Spin-flavor indices are suppressed in Eq. (4.12).]

The overlap properties of two-baryon states are obtained by computing the overlap:

$$\langle B(p_1)B(p_2)|B(p_3)B(p_4)\rangle\ ,$$

in which p_i labels the momentum and magnetic quantum numbers. The geometric aspects of computing the B-B overlap are more complicated than for meson-meson overlap. However, the result that the overlap function is the same as for elementary identical baryons emerges from the same assumptions. To see this is to begin by observing that

$$[U(\omega,\mathbf{x}_2,c_2)b^-(\mathbf{x}_2)]^r[U(\omega,\mathbf{x}_3,c_3)b^+(\mathbf{x}_3)]^s\epsilon^{rst}$$

have the color transformation properties of an antiquark (t) at ω. Then use the mesonic derivation. This is not necessary. One can also assume that the electric field vectors lie on the vectors $\mathbf{r}_i-\mathbf{R}$. If the strong coupling expansion is valid and flux tubes are narrow, one can obtain the result

$$\langle B(p_1)B(p_2)|B(p_3)B(p_4)\rangle=\delta_{p_1,p_3}\delta_{p_2,p_4}-\delta_{p_1p_4}\delta_{p_3,p_2}\ . \tag{4.13}$$

Similarly one may show that

$$\langle B(p_1)|B(p_2)M(p_3)\rangle=0 \tag{4.14a}$$

and

$$\langle B(p_1)M(p_4)|B(p_2)M(p_3)\rangle=\delta(\mathbf{p}_3-\mathbf{p}_4)\delta(\mathbf{p}_1-\mathbf{p}_2)\ . \tag{4.14b}$$

Eq. (4.14a) follows immediately from the lack of an antiquark in the baryon wave functions. That the flux line joining the $q\bar{q}$ pair of meson p_3 must be contiguous with the one of meson p_4 gives (4.14b). Equation (4.14) is assumed in the standard meson-baryon dynamics.

A. Effects of vacuum correlations

Both quark and gluon condensation occur in the QCD vacuum (eigenstate of lowest energy). Here the latter is considered. The dressing of the bare vacuum by plaquettes causes a nonzero expectation value of the square of the color-magnetic field. The physical vacuum $|\Omega\rangle$ is related to the bare vacuum $|0\rangle$ by

$$|\Omega\rangle=\left[1+\frac{1}{-\Lambda H\Lambda}\Lambda H_M\right]|0\rangle\ , \tag{4.15}$$

where $\Lambda=1-|0\rangle\langle 0|$ and the energy of the state Ω is chosen to be zero. Thus, $\langle\Omega|U_p|\Omega\rangle$ does not vanish. In SCQCD this matrix element is of order $1/g^4$; and therefore very small. However, SCQCD does not reliably predict glueball properties, so other techniques to estimate $\langle\Omega|U_p|\Omega\rangle$ must be used.

Consider the implications of the gluonic structure of the vacuum for the overlap term of Fig. 5(a). Take each side of the square to have length a. After the fermion contractions are made, one is left with four flux lines forming a plaquette U_{p_1}, Fig. 6(a).

The matrix element $\langle 0|U_{p_1}|0\rangle$ vanishes, but $\langle\Omega|U_{p_1}|\Omega\rangle$ does not. Thus, there *is* a nonvanishing quark-exchange term. However, the matrix element $\langle\Omega|U_p|\Omega\rangle$ is not likely to be unity so that one does not expect to reproduce the conventional quark exchange (QE) terms. One multiplies this matrix element by the appropriate factors as in (4.8) to evaluate the overlap $\mathcal{O}_G$.

In the following, I estimate the influence of vacuum correlations for the term of Fig. 5(a). The conventional QE term is multiplied by $\langle\Omega|U_{p_1}|\Omega\rangle$. This can be related to results of QCD sum rules.[30] One knows

$$\langle\Omega|B^2|\Omega\rangle=(600\ \text{MeV})^4\ . \tag{4.16}$$

The relationship between B^2 and plaquettes is

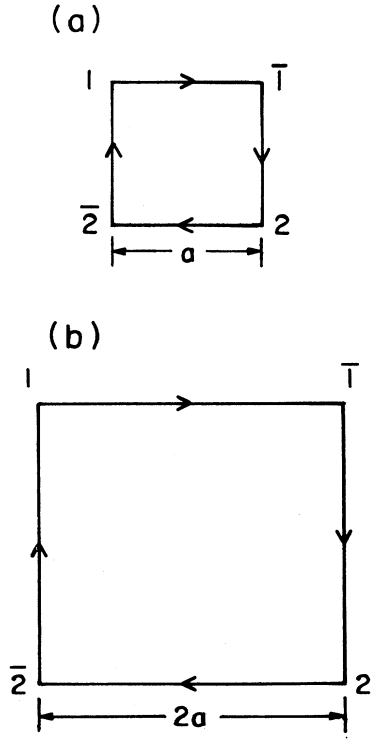

FIG. 6. Vacuum contributions to quark exchange given by expectation values of $U(c)$. (a) single plaquette term, (b) four plaquette term.

$$\langle\Omega|\int d^3x B^2|\Omega\rangle=\frac{-1}{g^2a}\langle\Omega|\sum_p(U_p+U_p^\dagger)|\Omega\rangle_c\ , \tag{4.17}$$

where the subscript c denotes connected matrix elements.

Consider the expectation value of just one plaquette. Use the translational invariance of the vacuum ($\langle\Omega|B^2|\Omega\rangle$ and $\langle\Omega|U_p|\Omega\rangle_c$ are independent of position) on both sides of (4.17). Then,

$$\langle\Omega|B^2|\Omega\rangle V=-\frac{N_p}{g^2a}\langle\Omega|U_{p_1}|\Omega\rangle_c=-\frac{N_p}{g^2a}\langle\Omega|U_{p_1}^\dagger|\Omega\rangle_c. \tag{4.18}$$

In (4.18), V is the volume of space and N_p is the number of plaquettes (squares of side a) on the $N\times N\times N$ lattice. For large N_p one has $N_p=3N^3=3V/a^3$, so

$$\langle\Omega|U_{p_1}|\Omega\rangle_c=-\frac{g^2a^4}{3}\langle\Omega|B^2|\Omega\rangle\ . \tag{4.19}$$

To evaluate the quark-exchange effect we need to know values of g and a. It is reasonable to take $g\approx 2$ so that $a\approx 0.2$ fm.[31] Using these, along with Eq. (4.16), gives

$$\langle\Omega|U_{p_1}|\Omega\rangle_c\approx\tfrac{1}{6}\ . \tag{4.20}$$

Recall that a vanishing result corresponds to elimination of QE terms, and that the value assumed in Pauli antisymmetrization is $+1$. Thus the result (4.20) implies a strong suppression of QE; furthermore even the sign is *opposite* to the conventional value. Thus conventional quark exchange may be erroneous.

Next I argue that even a magnitude of $\frac{1}{6}$ is likely to be an overestimate. This is because the single plaquette term of Eq. (4.20) is relevant only if all fermions are close together. [Recall Eq. (4.8).] This occurs with a limited probability. Cases in which the separation of the fermions is controlled by several plaquettes, as in Fig. 6(b), occur far more frequently. In that example, one needs the expectation of $U(c)$ as where c is the closed path around the perimeter of a square of are $4a^2$, Fig. 6(b). The expectation value of a plaquette of area $A=(TR)$ is given by the Wilson loop

$$W=\langle\Omega|U(c)|\Omega\rangle\ , \tag{4.21a}$$

$$W(A)=Ce^{-\sigma A}\ . \tag{4.21b}$$

in which T is a Euclidean time separation. I assume that it is valid to replace T by a spatial separation. Then the $U(c)$ expectation values for two areas A_1 and A_2 are related by

$$\frac{W(A_2)}{W(A_1)}=\exp[-\sigma(A_2-A_1)] \tag{4.22}$$

Since our case of interest has $A_2>A_1$ [compare Figs. 6(a) and (b)], the general overlap $|\langle\Omega|U_c|\Omega\rangle|$ is significantly less than $\frac{1}{6}$.

The present estimate is only a first examination of gluonic suppression. The g^2a^4 dependence of (4.19) indicates the crude nature of the result. More work will be needed to firmly settle the question. However, the present result is that QE effects are negligible.

B. Summary of Pauli principle result

The arguments presented earlier indicate that the exchange terms are very small. This is because local gauge invariance (LGI) causes each of the standard quark direct and exchange terms to be multiplied by very different flux-tube overlaps (gluonic matrix elements). In the strong coupling approach, the many gluons in the wave function are confined in a narrow tube. The exchange term generally requires an overlap between two flux tubes pointing in different directions. Hence it is plausible that the exchange terms are small.

V. SCQCD AND HADRON-HADRON SCATTERING

The present intent is to work out the consequences of SCQCD for nuclear physics. Therefore scattering processes should be considered. An earlier publication[12] examined meson-meson scattering and found that flux tube rearrangement (FTR) terms, in which color electric field configurations are changed, provide only a small potential. Furthermore, it was argued that string-breaking effects involving quark-pair creation are far more important than FTR.

This result is very different from the string flip-flop model[32] and other approaches[33] based on the use of adiabatic potential surfaces. Here a specific scattering problem is used to investigate the difference. The string flip-flop model is recovered only by neglecting the quark kinetic energy operator.

The contrast between SCQCD and the string flip-flop model is then emphasized by comparing two calculations[34,35] made in $1+1$ space-time dimensions. Thus the string flip-flop model is not a consequence of SCQCD.

A. A scattering problem

Turn to an example for meson-meson elastic scattering. Nonrelativistic kinematics are used. As a further simplification, consider channels for which the distinguishable quarks and antiquarks all have the same mass. (An example is $\pi^+-\pi^-$ (or $u\bar{d},d\bar{u}$) interactions.)

Start with a simplified Hamiltonian in which only the quark kinetic energy (T) and the electric energy term, H_E are included. Call $T+H_E=H_0$. Since T does not cause FTR and H_B is not included, the flux tube between a $q\bar{q}$ pair in a meson is a straight line. Then H_0 can be written as

$$H_0=\sum_i\frac{p_i^2}{2m}+\frac{\sigma}{2}\sum_{i,j}r_{i\bar{j}}\mathcal{O}_{i\bar{j}}\ . \tag{5.1}$$

$\mathcal{O}_{i\bar{j}}=1$ if there is a flux line between a quark i and antiquark $\bar{j}$. If no flux line between i and $\bar{j}$ exists, $\mathcal{O}_{i\bar{j}}=0$.

Now consider the plane-wave states. These consist of a direct product of a bound state wave function for each $q\bar{q}$ meson multiplied by a plane-wave factor. Such states are written using a first-quantized formulation, in which the quarks and antiquarks in one meson are labeled $1\bar{1}$ and in the other by $2\bar{2}$, Fig. 7(a). An alternate would be $1\bar{2}$ and $2\bar{1}$, Fig. 7(b). Denote the two possibilities of Fig. 7 as $|\phi_1\rangle$ and $|\phi_2\rangle$. The states $|\phi_1\rangle$ and $|\phi_2\rangle$ represent prod-

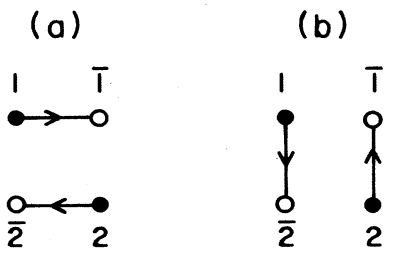

FIG. 7. Meson-meson scattering configurations.

ucts of two mesonic bound states. Furthermore, the plane-wave states $|\phi_{1,2}\rangle$ depend on the relative momentum e.g., $|\phi_{1,2}(\mathbf{p})\rangle$. Then,

$$|\phi_1(\mathbf{p})\rangle \equiv |M_{1\bar{1}}(\mathbf{p})\rangle \otimes |M_{2\bar{2}}(-\mathbf{p})\rangle \ , \tag{5.2a}$$

$$|\phi_2|\mathbf{p})\rangle \equiv |M_{1\bar{2}}(\mathbf{p})\rangle \otimes |M_{2\bar{1}}(-\mathbf{p})\rangle \ , \tag{5.2b}$$

in which $|M_{i\bar{m}}(\mathbf{p})\rangle$ is given by Eq. (4.4) or its continuum limit. As discussed in Sec. IV, the states $|\phi_i(\mathbf{p})\rangle$ obey the overlap property

$$\langle \phi_i(\mathbf{p}')|\phi_j(\mathbf{p})\rangle = \delta(\mathbf{p}-\mathbf{p}')\delta_{ij} \ . \tag{5.3}$$

It is necessary to examine the influence of H_0 on a single bound state. This is

$$\left[\frac{p_i^2+p_{\bar{m}}^2}{2m}+\sigma r_{i\bar{m}}\right]|M_{i\bar{m}}(\mathbf{p})\rangle \equiv h_0(i\bar{m})|M_{i\bar{m}}(\mathbf{p})\rangle = \left[\frac{p^2}{2M_{i\bar{m}}}+M_{i\bar{m}}\right]|M_{i\bar{m}}(\mathbf{p})\rangle, \tag{5.4}$$

in which $M_{i\bar{m}}$ is the meson mass, and quark i and antiquark m are joined by a flux line in $|M_{i\bar{m}}(\mathbf{p})\rangle$.

Now consider how H_0 [of Eq. (5.1)] affects $|\phi_1(\mathbf{p})\rangle$. The key point is that the operators $\mathcal{O}_{1\bar{1}}$ and $\mathcal{O}_{2\bar{2}}$ act on the existing flux lines. Hence,

$$\mathcal{O}_{1\bar{1}}, \mathcal{O}_{2\bar{2}} \to 1 \ . \tag{5.5a}$$

On the other hand, when H_0 acts on $|\phi_1(\mathbf{p})\rangle$ there is no flux line between quark 1 and antiquark $\bar{2}$. Hence $\mathcal{O}_{1\bar{2}}$ (and also $\mathcal{O}_{2\bar{1}}$) vanishes:

$$\mathcal{O}_{1\bar{2}}, \mathcal{O}_{2\bar{1}} \to 0 \ . \tag{5.5b}$$

The use of (5.5) simplifies $H_0|\phi_1(\mathbf{p})\rangle$:

$$H_0|\phi_1(\mathbf{p})\rangle = \left[\sum \frac{p_i^2}{2m}+\sigma(|\mathbf{r}_1-\mathbf{r}_{\bar{1}}|+|\mathbf{r}_2-\mathbf{r}_{\bar{2}}|)\right]|\phi_1(\mathbf{p})\rangle = \left[\frac{p^2}{2\mu_1}+M_{1\bar{1}}+M_{2\bar{2}}\right]|\phi_1(\mathbf{p})\rangle \ , \tag{5.6}$$

in which (5.4) is used to write the last line, and μ_1 is the reduced mass.

The meaning of (5.6) is clear. The confining potential H_E, when combined with the quark kinetic energy, does not cause scattering.

What then is the cause of scattering? Consider the magnetic term H_M which (Fig. 8 and Ref. 12) generates a flux-tube rearrangement. There is a nonzero matrix element connecting $|\phi_1(\mathbf{p})\rangle$ to the state $|\phi_2(\mathbf{p})\rangle$.

The relevant matrix element for scattering is obtained by inserting H_M [recall Eq. (2.16)] between $|\phi_1(\mathbf{p})\rangle$ and $|\phi_2(\mathbf{p})\rangle$. Define

$$V(\mathbf{p},\mathbf{p}') = \langle \phi_1(\mathbf{p})|H_M|\phi_2(\mathbf{p}')\rangle \ . \tag{5.7}$$

For this problem, the interaction between mesons may be represented as elements of an off-diagonal matrix $\hat{V}$,

$$\hat{V} = \begin{bmatrix} 0 & V \\ V & 0 \end{bmatrix} , \tag{5.8}$$

where, for example, the (1,2) element of the matrix represents the term of Eq. (5.7). The transition matrix $\hat{T}$ is given by the Lippmann-Schwinger (LS) equation

$$\hat{T} = \hat{V} + \hat{V}G_0\hat{T} \ , \tag{5.9}$$

where G_0 is the usual nonrelativistic propagator $G_0^{-1} = E + i\epsilon - k_1 - k_2$ where k_i are the mesonic kinetic energy operators and E is the total kinetic energy.

It is not my purpose here to estimate $\hat{T}$. It is sufficient to point out that H_M as represented in Eq. (5.7) by V causes the scattering. The scattering phase shifts depend on V.

B. Relationship with the string flip-flop model

Let's recover the string flip-flop model (SFFM). Simply neglect the quark kinetic energy T. Then the energy of a system formed by connecting quark 1 with antiquark T and connecting (quark) 2 with (antiquark) $\bar{2}$ is $\sigma(r_{1\bar{1}}+r_{2\bar{2}})$. If 1 and $\bar{2}$ are connected we have an energy $\sigma(r_{1\bar{2}}+r_{2\bar{1}})$. These are two possible eigenenergies. If one assumes that nature chooses the lowest energy configuration the energy is given by

$$\sigma \ \min(r_{1\bar{1}}+r_{2\bar{2}}, r_{1\bar{2}}+r_{2\bar{2}}) \ .$$

Equating this energy with a scattering potential leads to the string flip-flop potential energy.

In the simplest case,[36] there are two potential energy surfaces, one given by $\sigma(r_{1\bar{1}}+r_{2\bar{2}})$ and the other by $\sigma(r_{1\bar{2}}+r_{2\bar{1}})$. These levels would cross, but the H_M term causes transitions between the two states and flux-tube configurations of Figs. 7(a) and (b) push the levels apart.

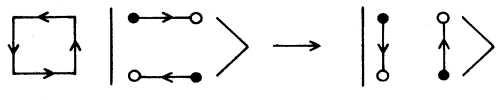

FIG. 8. Magnetic (H_B) contribution to meson-meson interaction ($H_B = H_M$).

(The idea is that H_M is small, but important compared to the vanishing energy gap.) Then a typical SFFM assumption is that one may use

$$\sigma \min(r_{1\bar{1}}+r_{2\bar{2}}, r_{1\bar{2}}+r_{2\bar{1}})$$

as a potential energy. Assuming an initial boundary condition allows the computation of phase shifts. However, these do not depend on H_M, in contrast with the results of Sec. VI A above.

The problem with the arguments for the string flip-flop model is that the kinetic energy T is neglected. As shown in Eq. (5.4), T combined with the linear potential produces a constant. Thus the eigenenergy is neither $\sigma(r_{1\bar{1}}+r_{2\bar{2}})$ nor $\sigma(r_{1\bar{2}}+r_{2\bar{1}})$.

The net result is that if one treats the quark kinetic energy and confining potential on the same footing, the string flip-flop model does not emerge from SCQCD.

C. Two-dimensional gauge theory

Another example of the difference between the string flip-flop model and QCD can be seen by comparing two calculations made in 1 space and 1 time dimension. In the work of Nambu and Bambah,[34] the interaction Hamiltonian for SU(3) gauge theory (QCD) is

$$H=-\frac{g^2}{8}\sum_{k,l}\bar{\lambda}^k\cdot\bar{\lambda}^l|x_k-x_l| \ . \tag{5.10}$$

In the string flip-flop model of Horowitz *et al.*,[35]

$$H=\min_{\{P\}}\sum_{n=1}^{N} v(|x_{P(2n-1)}-x_{P(2n)}|) \ , \tag{5.11}$$

in which the minimum is taken over all permutations P of quark labels pairing the N quarks into $N/2$ pairs. Suppose

$$v(|x_k-x_l|)=|x_k-x_l| \ .$$

Even then, the contrast between the QCD result (5.8) of Nambu and Bamba and the string flip-flop model (5.11) is quite clear. The two interactions have a very different form because of the influence of color contained in the $\lambda^k\cdot\lambda^l$ term.

D. Flux-tube rearrangement in baryon-baryon scattering

Begin by recalling the earlier estimate for s-wave meson-meson scattering.[12] The FTR contribution to the potential $V(\mathbf{p},\mathbf{p}')$ acts as a nonlocal potential between mesons. However, the results can be parametrized roughly by a typical local Yukawa potential $Y(r)$ of range $1/m$:

$$Y(r)=-Y_0\frac{e^{-mr}}{mr} \ . \tag{5.12}$$

where $Y_0\approx 10^{-1}$ MeV with $m=2m_\pi$. This is very small indeed, since typical strong interaction potentials are of the order of tens of MeV at least. Thus the flux-tube rearrangement term seems to be negligible in meson-meson scattering.

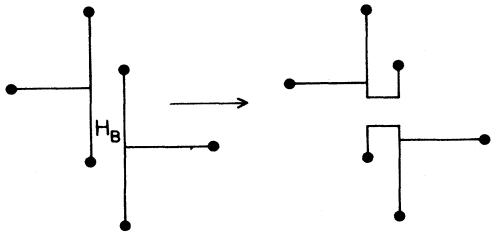

FIG. 9. Typical contribution to flux-tube rearrangement effects in baryon-baryon scattering.

Turn now to baryons. A typical contribution due to flux-tube rearrangement is shown in Fig. 9. These terms are of order $1/g^6$ or higher. This is because the FTR leads to color electric field configurations that are wave function admixtures of order $1/g^2$. There is one such factor for each of the two-baryon wave functions and another for the interaction V. The perturbation series for V seems to converge rapidly[12] when expanded in powers of $1/g^2$. Thus flux-tube rearrangement seems even smaller for baryons than for mesons.

The preceding result is that flux-tube rearrangement terms are very much smaller than typical strong interactions. It is then necessary to determine the origin of hadron-hadron scattering. Terms most like the conventional mesonic exchange description arise from string breaking.[12] See Fig. 10, for examples. In general, many

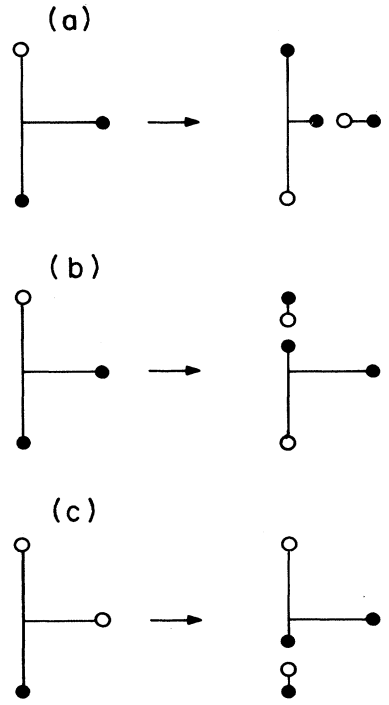

FIG. 10. Emission of pairs by the string-breaking mechanism.

different links can be broken. This enhances the likelihood for string breaks to occur.

VI. STRING-BREAKING TREATMENT OF MESON DECAY AND MESON EMISSION FROM BARYONS

It seems (from Sec. V) that string-breaking quark-pair creation (QPC) is an important ingredient in the interactions between hadrons. Here I estimate the QPC contribution to the meson-nucleon coupling constant using the QPC operator of Kokoski and Isgur (KI).[13] Those authors found that the QPC operator can be well approximated by one of the form of the $^3P_0$ model.[37] This is discussed next.

A. Effective pair production operator

KI use the locally gauge invariant "naive" quark kinetic energy term K, with

$$K=\frac{1}{a}\sum_{e_{ji}} q_j^\dagger U_{ji}\alpha_{ji}q_i \ , \tag{6.1}$$

where q_n is the quark field operator at lattice site n, U_{ji} creates a unit of color SU(3) flux on the link from j to i and α_{ji} is the component of the Dirac matrix in the direction of the link from j to i. When a meson flux tube is broken by quark-pair creation on a link from $\mathbf{x}$ to $\mathbf{x}+a\hat{\mathbf{e}}$, the resulting quark pair is created with an effective operator

$$H_{\rm QPC}=\sum_{\mathbf{x},e} q^\dagger(\mathbf{x})\boldsymbol{\alpha}\cdot\hat{\mathbf{e}}q(\mathbf{x}+a\hat{\mathbf{e}})\frac{9\gamma(\mathbf{x},\hat{\mathbf{e}})}{3a} \ . \tag{6.2}$$

The function $9\gamma(\mathbf{x},\hat{\mathbf{e}})$ is the overlap between the initial color flux state of the initial meson and that of the final two-meson state. KI assume that $\gamma(\mathbf{x},\hat{\mathbf{e}})$ is independent of the direction $\hat{\mathbf{e}}$; treat a as small; and, take $\hat{\mathbf{e}}$ to point in random directions. Then,

$$H_{\rm QPC}\approx\sum_{\mathbf{x}} q^\dagger(\mathbf{x})\boldsymbol{\alpha}\cdot\nabla q(x)\gamma(\mathbf{x}) \ . \tag{6.3}$$

KI start with Eq. (6.3) and make numerical studies of different models of $\gamma(\mathbf{x})$. They show that it is a good approximation to treat γ as a constant. The use of the resulting QPC operator then leads to a very good description of all the decays $M\to m_1m_2$.

The assumption that $\hat{\mathbf{e}}$ is randomly oriented contrasts with the notion of linear flux tubes. However, QPC depends on short distance effects, while the linear flux tube is thought to be more valid at larger separations. Phenomenology of meson decay supports the random nature of $\hat{\mathbf{e}}$. If one takes $\hat{\mathbf{e}}$ to be parallel to the flux line, one obtains the so-called $^3S_1$ model which disagrees[13] with the decay rate for $B\to\omega\pi$. See, however, Ref. 14.

It is useful to incorporate a correct description of the mesonic decays in a treatment of the meson-nucleon coupling constants, so we use the KI operator $H_{\rm QPC}$ in this first evaluation of meson-baryon coupling constants.

The effective Hamiltonian (with γ constant) is

$$H_{\rm QPC}=\gamma\int d^3x q^\dagger(\mathbf{x})\boldsymbol{\alpha}\cdot\nabla q(x) \ , \tag{6.4}$$

which is the $^3P_0$ model.[37,38] I proceed by using the γ obtained from the decay $\rho\to\pi\pi$ in computing some meson-baryon coupling constants.

The first step is to rewrite Eq. (6.4) in second quantized notation,

$$H_{\rm QPC}=\int d^3k d^3k'\delta(\mathbf{k}''+\mathbf{k}')\gamma\sum_m \langle 1m\,1-m|00\rangle\mathcal{Y}_1^m(\mathbf{k}''-\mathbf{k}')\times\frac{1}{\sqrt{3}}\sum_{tm_1} b^\dagger_{m_1t}(\mathbf{k}'')a^\dagger_{m_2-t}(\mathbf{k}')\langle\tfrac{1}{2}m_1\tfrac{1}{2}m_2|1-m\rangle\langle\tfrac{1}{2}t\tfrac{1}{2}-t|00\rangle \ , \tag{6.5}$$

in which the operator $b^\dagger(a^\dagger)$ creates antiquarks (quarks). Factors arising from counting of colors are the same for the terms $\rho\to\pi\pi$ and $N\to N\pi$, and are therefore absorbed into the constant γ.

B. The decay $\rho\to\pi\pi$

We first compute the amplitude $\mathcal{M}_{\rho\to\pi\pi}$,

$$\mathcal{M}_{\rho\to\pi\pi}=\langle\pi(\mathbf{k}_1)\pi(\mathbf{k}_2)|H_{\rm QPC}|\rho\rangle \ . \tag{6.6}$$

The application of $H_{\rm QPC}$ of Eq. (6.5) yields

$$M_{\rho\to\pi\pi}=\frac{\gamma\delta(\mathbf{k}_1+\mathbf{k}_2)}{6}\left[\frac{3}{4\pi}\right]^2\mathbf{k}_1\cdot\hat{\boldsymbol{\rho}}F(k_1) \ , \tag{6.7a}$$

$$\equiv\delta(\mathbf{k}_1+\mathbf{k}_2)A \tag{6.7b}$$

in which $\hat{\boldsymbol{\rho}}$ is the spin direction of the ρ meson in its rest frame, and

$$F(k)=\int d^3p\left[1-\frac{2\mathbf{p}\cdot\mathbf{k}}{k^2}\right]\psi_\pi^2(p)\psi_\rho(|\mathbf{p}+\mathbf{k}/2|) \ . \tag{6.8}$$

The momentum arguments appearing in (6.8) are the usual canonical momenta.

It is convenient to relate $\mathcal{M}_{\rho\to\pi\pi}$ to the constant $f_{\rho,\pi\pi}$ of the covariant notation

$$\mathcal{H}=f_{\rho\pi\pi}(\boldsymbol{\pi}\times\partial^\mu\boldsymbol{\pi})\cdot\boldsymbol{\rho} \ . \tag{6.9}$$

Then

$$\mathcal{M}^{cv}=\int d^3r\langle\rho|\mathcal{H}|\pi(k_1)\pi(k_2)\rangle=\frac{(2\pi)^3\delta(\mathbf{k}_1+\mathbf{k}_2)2\pi\delta(E_i-E_f)f_{\rho\pi\pi}2i\mathbf{k}_1\cdot\hat{\boldsymbol{\rho}}}{\sqrt{2M_\rho}\sqrt{2\omega_1}\sqrt{2\omega_2}(2\pi)^{9/2}} \ , \tag{6.10}$$

in which $\mathcal{M}^{cv}$ is the covariant amplitude. This leads to a transition rate

$$W=\frac{k_1^3 f_{\rho\pi\pi}^2}{4\pi M_\rho^2}\frac{2}{3} . \tag{6.11}$$

The experimental value of W is 154±5 MeV, giving $f_{\rho\pi\pi}=6.1$. To relate $f_{\rho\pi\pi}$ to $\mathcal{M}_{\rho\to\pi\pi}$, simply remove the factor $2\pi\delta(E_i-E_f)$ from the right-hand side of Eq. (6.10) and equate the remainder with Eq. (6.7). This gives

$$f_{\rho\pi\pi}=\gamma M_\rho^{3/2}F(k_1)\pi\frac{\sqrt{3}}{6} . \tag{6.12}$$

The use of the relativistic formulae of (6.10) and (6.11) is the same as using relativistic phase space factors "golden rule" expression

$$W=2\pi\int|\langle\pi\pi|\bar{H}_{\rm QPC}|\rho\rangle|^2\frac{k_1E_\pi^2(k_1)|A|^2}{M_\rho}d\Omega_1 . \tag{6.13}$$

Indeed, the use of (6.7b) in (6.13) leads to the result (6.11), if the identification (6.12) is made.

The use of a relativistic phase space along with a nonrelativistic calculation has been questioned.[13,14] If the nonrelativistic phase space is used, the factor $E_\pi^2(k_1)$ is replaced by m_π^2. Thus, using the nonrelativistic phase space is the same as reducing the right-hand side of (6.18) by a factor of $m_\pi^2/(m_\rho^2/4)$. Kokoski and Isgur use a prescription in which the factor $E_\pi^2(k_1)/M_\rho$ is replaced by $\tilde{m}_\pi\tilde{m}_\pi/\tilde{m}_\rho$, where $\tilde{m}_\pi=\tilde{m}_\rho=0.72$ GeV is the calculated meson mass in the spin independent potential. This factor is meant to incorporate recoil in the weak binding limit. The use of $\tilde{m}_\pi\tilde{m}_\pi/\tilde{m}_\rho$ in Eq. (6.13) instead of $E_\pi^2(k_1)/M_\rho$ is equivalent to multiplying Eq. (6.13) by a factor $0.72/0.19\approx3.7$. There is a factor of 5.1 difference between the γ obtained via the KI prescription and the use of nonrelativistic phase space advocated by Kumano and Pandharipande[14] (KP). Note that the ambiguities are worse for the case $\rho\to\pi\pi$ than for the other meson decays. We return to the question of relativistic problems.

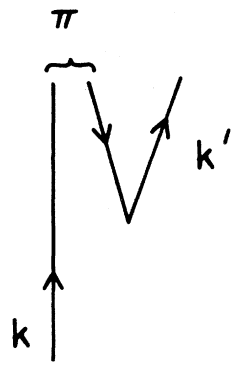

FIG. 11. Matrix element for a quark of momentum k to emit a pion and become a quark of momentum k'.

C. πNN coupling constant

The calculation is simplified by first using $H_{\rm QPC}$ [Eq. (6.5)] to evaluate the matrix element for pionic emission by a quark, $\hat{\mathcal{O}}_\pi$, see Fig. 11. Then the matrix element of the single quark operator $\hat{\mathcal{O}}_\pi$ is evaluated between initial and final nucleon states. This can be done because Pauli exchange terms between the π and N are suppressed, and gluonic overlaps are incorporated in the constant γ.

The operator $\hat{\mathcal{O}}_\pi$ which describes the emission of a pion of momentum and isospin q by a nucleon of momentum, spin and isospin P_i is defined by

$$\langle\pi(q)N(P_f)|\hat{\mathcal{O}}_\pi|N(P_i)\rangle\equiv\langle\pi(q)N(P_f)|H_{\rm QPC}|N(P_i)\rangle , \tag{6.14}$$

where

$$\hat{\mathcal{O}}_\pi=\int dq\,dk\,dk'\,A_\pi^\dagger(q)a_{m_ft_f}^\dagger(\mathbf{k}')a_{m_it_i}(\mathbf{k})\langle\pi(q)k'|H_{\rm QPC}|k\rangle , \tag{6.15}$$

in which q,k,k' stand for momentum, flavor, and spin indices. In particular ($k\equiv\mathbf{k}m_it_i$).

To proceed, we need a model of the pion creation operator $A_\pi^\dagger(q)$. The ones of Refs. 10 (GI) and 9 (CKP) are used here. Thus, I write

$$A_\pi^\dagger(q)=\sum_{m'm''t't''}a_{m't'}^\dagger(\mathbf{K}+\mathbf{q})b_{m''t''}^\dagger(-\mathbf{K})\phi_\pi(|\mathbf{K}-\mathbf{q}/2|)\langle\tfrac{1}{2}m'\tfrac{1}{2}m''|00\rangle\langle\tfrac{1}{2}t'\tfrac{1}{2}t''|1t_z\rangle . \tag{6.16}$$

Note that the use of the chirally symmetric staggered-Fermion Hamiltonian of Eq. (2.27) indicates that the Nambu-Jona Lasinio mechanism is present. A more complicated BCS-type pion wave function would then emerge. The application of Eq. (2.27) is left for the future.

Next evaluate

$$\langle\pi(q)k'|H_{\rm QPC}|k\rangle$$

using Eq. (6.5) and the standard relations

$$|k\rangle=a_{mt}^\dagger(\mathbf{k})|0\rangle$$

and

$$|\pi(q)\rangle = A_\pi^\dagger(q)|0\rangle \ .$$

The result is

$$\langle \pi(q)k'|H_{\rm QPC}|k\rangle = \frac{-\delta(\mathbf{k}'-\mathbf{k}+\mathbf{q})}{4\sqrt{3\pi}}\gamma(\tfrac{1}{2}m_f\tfrac{1}{2}t_f|\boldsymbol{\sigma}\cdot(\mathbf{q}-\mathbf{k})\boldsymbol{\tau}\cdot\hat{\boldsymbol{\phi}}|\tfrac{1}{2}m_i t_i\rangle\phi_\pi\left(\left|\mathbf{k}-\frac{\mathbf{q}}{2}\right|\right) . \tag{6.17}$$

The main difference between (6.17) and treatments in which the pion is treated as an elementary object is the magnitude of the term proportional to the quark's initial momentum [$\mathbf{k}$, not $\mathbf{k}\omega(q)/m$] and the appearance of the pion wave function.

Turn next to the computation of the πNN coupling constant. This requires evaluation of (6.14) with the specific matrix elements (6.15) and (6.17). To begin, note that the nucleon state vector of total momentum P can be written (suppressing indices) as

$$|N(P)\rangle = \delta\left(\mathbf{P}-\sum_{j=1}^{3}\mathbf{P}_j\right)\psi_N(P_\rho,P_\lambda)a^\dagger(P_1)a^\dagger(P_2)a^\dagger(P_3)|0\rangle \equiv \delta\left(\mathbf{P}-\sum_{j=1}^{3}\mathbf{P}_j\right)|N\rangle \ , \tag{6.18}$$

with

$$\begin{aligned}\mathbf{P}_\rho &= \frac{\mathbf{P}_1-\mathbf{P}_2}{\sqrt{2}} \ , \\ \mathbf{P}_\lambda &= \frac{\mathbf{P}_1+\mathbf{P}_2-2\mathbf{P}_3}{\sqrt{6}} \ .\end{aligned} \tag{6.19}$$

The use of (6.18), (6.17), and (6.19) in (6.23) yields

$$\langle \pi(q)N(P_f)|H_{\rm QPC}|N(P_i)\rangle = -\frac{\gamma}{4\sqrt{3\pi}}\delta(\mathbf{P}_i-\mathbf{q}-\mathbf{P}_f)\langle N|\sum_{j=1,3}e^{-i\mathbf{q}\cdot\boldsymbol{\tau}_j}\boldsymbol{\sigma}_j\cdot(\mathbf{q}-\mathbf{P}_j)\boldsymbol{\tau}_j\cdot\hat{\boldsymbol{\phi}}\phi_\pi\left(\left|\frac{\mathbf{q}}{2}-\mathbf{P}_j\right|\right)|N\rangle \ . \tag{6.20}$$

In evaluating (6.20), the momentum operators $\mathbf{P}_j$ are to be expressed in terms of $\mathbf{P}_\rho$ and $\mathbf{P}_\lambda$ with $\sum_j \mathbf{P}_j = 0$. Next use symmetry considerations to simplify (6.20). The matrix element appearing on the right-hand side of (6.20) is a function of $|\mathbf{q}|=q$ times the matrix element of $\boldsymbol{\sigma}_N\cdot\mathbf{q}\boldsymbol{\tau}_N\cdot\hat{\boldsymbol{\phi}}$, with N denoting an operator acting on the nucleon coordinates. We may thus define a quantity $F(q)$ such that

$$\langle \pi(q)N(P_f)|H_{\rm QPC}|N(P_i)\rangle = \delta(\mathbf{P}_i-\mathbf{q}-\mathbf{P}_f)F(q)\left[f\left|\boldsymbol{\sigma}_N\cdot\left[\mathbf{q}-\frac{P_i}{3}\right]\boldsymbol{\tau}_N\cdot\hat{\boldsymbol{\phi}}\right|i\right] \ , \tag{6.21}$$

where

$$|i(f)=|\tfrac{1}{2}m_{i(f)}\tfrac{1}{2}t_{i(f)}) \ .$$

The term $F(q)$ is defined by comparing (6.20) and (6.21) which are equivalent statements of the same quantity.

The result (6.21) is the one we seek. However to evaluate the πNN coupling constant $G_{\pi NN}$, one must compare Eq. (6.21) with standard forms. In conventional pseudoscalar (or pseudovector) theory one has

$$\langle \pi(q)N(P_f)|H^{\rm conv}|N(\mathbf{P}_i)\rangle = G_{\pi NN}\bar{u}(P_f)\gamma_5 u(P_i)\frac{V(q)}{\sqrt{2\omega_q}}\frac{1}{(2\pi)^{3/2}}(f|\boldsymbol{\tau}_N\cdot\hat{\boldsymbol{\phi}}|i)\delta(\mathbf{q}+\mathbf{P}_f-\mathbf{P}_i) \ , \tag{6.22}$$

in which $V(q)$ is the vertex function with $V(q=0)=1$, $\omega_q=(q^2+M^2)^{1/2}$, and the measured value of $G_{\pi NN}$ is 13.4. It is convenient to compare (6.20) and (6.22) in the frame in which $\mathbf{P}_i=0$. Then,

$$\bar{u}(P_i)\gamma_5 u(P_i) \approx \frac{\boldsymbol{\sigma}_N\cdot\mathbf{q}}{2M} \ , \tag{6.23}$$

with $u^\dagger u$ as unity and taking $(q/2M)^2 \ll 1$. The factors $V(q)$ and G are determined by comparing (6.2) (with $P_i=0$) and (6.20). The results are

$$G_{\pi NN} = 2M(2m_\pi)^{1/2}(2\pi)^{3/2}F(0) \tag{6.24}$$

and

$$V(q) = \frac{F(q)}{F(0)}\left[\frac{\omega_q}{m_\pi}\right]^{1/2} . \tag{6.25}$$

The use of KI kinematics modifies Eqs. (6.24) and (6.25) by the replacement $m_\pi^{1/2} \to \tilde{m}_\pi^{1/2}$. (Recall $\tilde{m}_\pi = 0.72$ GeV.) This is required to obtain the same treatment of pion kinematics for meson and baryon emission of pions.

The result (6.24) depends on the frame of reference. For example, using $\mathbf{P}_i = \mathbf{q}/2$ would lead to a version of (6.24) in which $F(0)$ would be replaced by $\frac{5}{6}F(0)$.

The πNN coupling constant $G_{\pi NN}$ and form factor $V(q)$ are each given in terms of known constants and the function $F(q)$. To proceed, I display formulae for $F(q)$ with different models of the nucleon wave function.

First consider the work of Carlson *et al.* in which the wave function is a spatially symmetric wave function times the SU(4) spin-isospin wave function, times the color antisymmetric term. Defining the corresponding function version of $F(q)$ [from (6.20) and (6.22)] as $F^{ss}(q)$, leads to

$$q^2 F^{ss}(q) = \frac{-\gamma}{4\sqrt{3\pi}} \frac{5}{3} \int d^3P_\rho d^3P_\lambda \psi^* \left[\mathbf{P}_\rho, \mathbf{P}_\lambda + \left[\frac{2}{3}\right]^{1/2} \mathbf{q} \right] \psi(\mathbf{P}_\rho, \mathbf{P}_\lambda) \left[q^2 + \left[\frac{2}{3}\right]^{1/2} \mathbf{q}\cdot\mathbf{P}_\lambda \right] \phi_\pi \left[\left| \frac{\mathbf{q}}{2} + \left[\frac{2}{3}\right]^{1/2} \mathbf{P}_\lambda \right| \right] . \tag{6.26}$$

Capstick and Isgur[11] use a different representation for computing baryon wave functions. Their calculations are simplified by taking states to be explicitly antisymmetric only under interchange of quarks one and two. For the proton, the components $|\alpha\rangle$ are

$$|\alpha\rangle = C_A |uud\rangle \otimes \sum_{M_L M_S} \langle LM_L SM_s | \tfrac{1}{2} M \rangle |LM_L, n_\rho l_\rho, n_\lambda l_\lambda\rangle |\delta, SM_s,\rangle , \tag{6.27}$$

where C_A is the color antisymmetric wave function. The index α is shorthand,

$$\alpha \equiv \{ L \delta n_\rho l_\rho n_\lambda l_\lambda \} .$$

The spatial wave function for the component $|\alpha\rangle$ is

$$\langle \mathbf{P}_\rho, \mathbf{P}_\lambda | LM_L, n_\rho l_\rho N_\lambda l_\lambda \rangle = \phi_{n_\rho l_\rho}(P_\rho) \phi_{n_\lambda l_\lambda}(P_\lambda) [Y_{l_\rho}(\hat{\mathbf{P}}_\rho) \otimes Y_{l_\lambda}(\hat{\mathbf{P}}_\lambda)]_{LM_L} , \tag{6.28}$$

in which ϕ_{nl} are harmonic oscillator wave functions. The index δ defines the spin wave functions, e.g.,

$$|2, \tfrac{1}{2}\tfrac{1}{2}\rangle = \frac{1}{\sqrt{6}} |2\uparrow\uparrow\downarrow - \uparrow\downarrow\uparrow - \downarrow\uparrow\uparrow\rangle . \tag{6.29}$$

The proton wave function is then given by

$$|N\rangle_{CI} = \sum_\alpha C(\alpha) |\alpha\rangle . \tag{6.30}$$

CI determine $C(\alpha)$ from a variational calculation.

The matrix element of (6.20) can be expressed as

$$\begin{aligned} \langle \pi(q) N(P_f) | H_{\rm QPC} | N(P_i) \rangle = & -\frac{\gamma}{4\sqrt{3\pi}} \delta(\mathbf{P}_i - \mathbf{q} - \mathbf{P}_f) \\ & \times {}_{CI}\langle N | \left[2 e^{-i\mathbf{q}\cdot\mathbf{r}_2} \boldsymbol{\sigma}_2 \cdot (\mathbf{q} - \mathbf{P}_2) \boldsymbol{\tau}_2 \cdot \hat{\boldsymbol{\phi}} \phi_\pi \left[\left| \frac{\mathbf{q}}{2} - \mathbf{P}_2 \right| \right] \right. \\ & \left. + e^{-i\mathbf{q}\cdot\mathbf{r}_3} \boldsymbol{\sigma}_3 \cdot (\mathbf{q} - \mathbf{P}_3) \boldsymbol{\tau}_3 \cdot \hat{\boldsymbol{\phi}} \phi_\pi \left[\left| \frac{\mathbf{q}}{2} - \mathbf{P}_3 \right| \right] \right] | N \rangle_{CI} \end{aligned} \tag{6.31a}$$

$$= -\frac{\gamma}{4\sqrt{3\pi}} \delta(\mathbf{P}_i - \mathbf{q} - \mathbf{P}_f) \langle P_f | (T_2 + T_3) | P_i \rangle . \tag{6.31b}$$

The expression (6.31b) introduces terms T_2 and T_3 representing the matrix element in (6.31a) that involves either the second or third quark. Next evaluate T_2 and T_3. A useful approximation is to keep only terms with $L = 0$ and $\delta = 2$. (This accounts for more than 98% of the wave function.) Then evaluating the diagonal matrix element of T_3 for a spin up proton ($|p\uparrow\rangle$) leads to

$$\begin{aligned} \langle p\uparrow | T_3 | p\uparrow \rangle = & \tfrac{1}{3} \sum_{\alpha\alpha'} C(\alpha') \delta(n_\rho, n'_\rho) \delta(l_\rho, l'_\rho) \delta(\delta, 2) \delta(L, 0) \delta(\delta', \delta) \delta(L, L') \\ & \times \int d^3\mathbf{P}_\lambda \left[q + \left[\frac{2}{3}\right]^{1/2} P_\lambda \right]_0 \phi_{n_\lambda l_\lambda}(P'_\lambda) \phi_{n'_\lambda l_\lambda}(P_\lambda) \phi_\pi \left[\left| \frac{\mathbf{q}}{2} + \left[\frac{2}{3}\right]^{1/2} \mathbf{P}_\lambda \right| \right] \frac{1}{4\pi} P_{l_\lambda}(\hat{\mathbf{P}}'_\lambda \cdot \hat{\mathbf{P}}_\lambda) , \end{aligned} \tag{6.32}$$

where $\mathbf{P}'_\lambda \equiv \mathbf{P}_\lambda + \sqrt{2/3}\mathbf{q}$ and the direction of the proton's spin is 0.

Evaluation of T_2 seems more complicated because $\mathbf{r}=-\boldsymbol{\rho}/\sqrt{2}+\boldsymbol{\lambda}/\sqrt{6}$ and all of the quarks are involved. However, we may define new spatial coordinates $\boldsymbol{\rho}'$ and $\boldsymbol{\lambda}'$ such that

$$\boldsymbol{\rho}'=\tfrac{1}{2}\boldsymbol{\rho}+\frac{\sqrt{3}}{2}\boldsymbol{\lambda}\ ,$$
$$\boldsymbol{\lambda}'=-\frac{\sqrt{3}}{2}\boldsymbol{\rho}+\frac{\boldsymbol{\lambda}}{2}\ . \tag{6.33}$$

With these, $\mathbf{r}_2=+\boldsymbol{\lambda}'\sqrt{2/3}$. This provides an important simplification because one can rewrite

$$\langle \mathbf{P}_\rho,\mathbf{P}_\lambda|LM_2,n_\rho l_\rho n_\lambda l_\lambda\rangle$$

in terms of $\boldsymbol{\rho}'$ and $\boldsymbol{\lambda}'$ using the Gal transformation.[39] Simply use Eq. (3.14) of Ref. 39 with the angle $\beta=-2\pi/3$. The nucleon can be rewritten

$$|N\rangle=\sum_\alpha C(\alpha)|\alpha\rangle=\sum_\beta D(\beta)|\beta\rangle\ , \tag{6.34}$$

in which the coordinate representation of the component $|\beta\rangle$ is $\langle\boldsymbol{\rho}',\boldsymbol{\lambda}'|\beta\rangle$. One finds

$$\langle p\uparrow|T_2|p\uparrow\rangle=\tfrac{4}{3}\sum_{\beta\beta'}D(\beta)D(\beta')\delta(n_\rho,n'_\rho)\delta(n_\lambda,n'_\lambda)\delta(\delta,2)\delta(L,0)\delta(L',0)\delta(\delta',2)$$
$$\times\int d^3P_\lambda\left[q+\left[\frac{2}{3}\right]^{1/2}P_\lambda\right]_0\phi_{n_\lambda l_\lambda}(P'_\lambda)\phi_{n'_\lambda l'_\lambda}(P_\lambda)\frac{1}{4\pi}P_{l\lambda}(\hat{\mathbf{P}}'_\lambda\cdot\hat{\mathbf{P}}_\lambda)\phi_\pi\left[\left|\frac{\mathbf{q}}{2}+\left[\frac{2}{3}\right]^{1/2}\mathbf{P}_\lambda\right|\right]\ . \tag{6.35}$$

These matrix elements of T_2 and T_3 can be used to compute the coupling constant and form factor [Eqs. (6.30)–(6.36)]

$$q_0F_{CI}(q)=\frac{-\gamma}{4\sqrt{3\pi}}\langle p\uparrow|T_2+T_3|p\uparrow\rangle\ . \tag{6.36}$$

D. The ωNN coupling constant

The quark-pair creation operator of Eq. (6.10) can also be used to compute the coupling constant between an ω meson (ω) and the nucleon. The procedure is essentially the same as in the preceding section.

First write the creation operator for an ω meson of spin projection M_v:

$$A^\dagger_\omega(\mathbf{q},M_v)=\sum_{m't'm''t''}a^\dagger_{m't'}(\mathbf{k}+\mathbf{q})b^\dagger_{m''f''}(-\mathbf{k})\phi_\omega(|\mathbf{k}-\mathbf{q}/2|)\langle\tfrac{1}{2}m'\tfrac{1}{2}m''|lM_v\rangle\langle\tfrac{1}{2}t'\tfrac{1}{2}t''|00\rangle\ . \tag{6.37}$$

Only three components of the vector meson's polarization vector are included. Next compute the $qq\omega$ vertex function. I find

$$\langle\omega(\mathbf{q},M_v)k'|H_{\rm QPC}|k\rangle=\phi_\omega(|\mathbf{k}-\mathbf{q}/2|)\delta(\mathbf{k}'+\mathbf{q}-\mathbf{k})\frac{\gamma}{4}\frac{1}{\sqrt{3\pi}}\langle\tfrac{1}{2}m_f|\mathbf{V}\cdot\hat{\boldsymbol{\epsilon}}_{M_v}+i(\boldsymbol{\sigma}\times\mathbf{V})\cdot\hat{\boldsymbol{\epsilon}}_{M_v}|\tfrac{1}{2}m_i\rangle\ , \tag{6.38}$$

where the initial (final) quark of momentum $\mathbf{k}(\mathbf{k}')$ has a spin $m_i(m_f)$ and $\mathbf{V}=\mathbf{q}-\mathbf{k}$. The matrix element of (6.38) can be rewritten as

$$\langle\omega(\mathbf{q},M_v)N(P_f)|H_{\rm QPC}|N(P_i)\rangle=\delta(\mathbf{P}_i-\mathbf{q}-\mathbf{P}_f)\hat{\boldsymbol{\epsilon}}_{M_v}\cdot\left\{3\left[\mathbf{q}-\frac{\mathbf{P}_i}{3}\right]+i(f|\boldsymbol{\sigma}_N|i)\times\left[\mathbf{q}-\frac{\mathbf{P}_i}{3}\right]\right\}F_\omega(|\mathbf{q}|)\ . \tag{6.39}$$

The quantity $F_\omega(|\mathbf{q}|)$ may be computed using (6.38). The factor 3 in (6.39) enters from the sum over three quarks.

To evaluate the ωNN coupling constant, compare Eq. (6.39) with the standard form

$$\langle\omega(\mathbf{q},M_v)N(P_f)|H^{\rm conv}|N(P_i)\rangle=\delta(\mathbf{P}_i-\mathbf{q}-\mathbf{P}_f)\frac{V_\omega(q)}{(2\pi)^{3/2}\sqrt{2}(q^2+m_\omega^2)^{1/2}}\hat{\boldsymbol{\epsilon}}\cdot\left[\frac{g_\omega}{2M}(\mathbf{P}_f+\mathbf{P}_i)+\frac{(f_\omega+g_\omega)}{2M}i\boldsymbol{\sigma}_N\times\mathbf{q}\right]\ . \tag{6.40}$$

This is the nonrelativistic reduction of standard expressions for vector coupling g_ω and tensor coupling f_ω.

One would like to compare Eqs. (6.40) and (6.39) to obtain g_ω and f_ω. However, the two equations have different forms, so a simple comparison is not possible. Our $^3P_0$ treatment does not reproduce the covariant omega-nucleon vertex. A less ambitious goal is to obtain f_ω and g_ω in the rest frame of the initial nucleon, $\mathbf{P}_i=0$. This is meaningful only if $q/M\ll1$. The results obtained by setting $\mathbf{P}_i=0$ are

$$g_\omega + f_\omega = \sqrt{2m_\omega}(2\pi)^{3/2} 2MF_\omega(0) ,$$
$$f_\omega/g_\omega = -\tfrac{2}{3} , \tag{6.41}$$
$$V_\omega(q) = \frac{F_\omega(q)}{F_\omega(0)} \left[\frac{q^2+m_\omega^2}{m_\omega^2} \right]^{1/4} .$$

This computed value of f_ω/g_ω disagrees with experiments which give ≈ 0. However, an equally likely choice $\mathbf{P}_f = 0$ would modify the first line of (6.41) only by a multiplicative factor of $\frac{2}{3}$ on the right-hand side. The ratio f_ω/g_ω would, however change to $+\frac{2}{3}$. Averaging the results would yield $f_\omega/g_\omega = 0$ and $f_\omega + g_\omega \propto \frac{5}{6}F(0)$ [instead of $F(0)$ as in (6.41)]. (It is reasonable to consider some kind of spread in $\mathbf{P}_i$ since nucleons in the centers of nuclei move isotropically.) In any case these examples show that f_ω/g_ω is more sensitive to $\mathbf{P}_i$ than $f_\omega + g_\omega$. In the following, I ignore the ratio and examine the sum as given (6.41).

An explicit evaluation of $g_\omega + f_\omega$ is made herein. It is useful to get a rough idea about $(g_\omega + f_\omega)/G_{\pi NN}$. With the standard proton spin-isospin wave function one finds

$$\frac{(g_\omega + f_\omega)}{G_{\pi NN}} = \frac{3}{5}\frac{F_\omega(0)}{F(0)} \left[\frac{m_\omega}{m_\pi} \right]^{1/2} , \tag{6.42a}$$

or

$$\frac{g_\omega + f_\omega}{G_{\pi NN}} = \frac{3}{5}\frac{F_\omega(0)}{F(0)} \left[\frac{m_\omega}{\tilde{m}_\pi} \right]^{1/2} , \tag{6.42b}$$

if KI kinematics is used. In any case, substantial ωNN coupling is obtained, assuming that the evaluation of $G_{\pi NN}$ leads to a value reasonably close to that of the experiments.

E. The ρNN coupling constant

The procedure is the same as for the ω meson, with only the isospin factors changing. The relevant matrix element is

$$\langle \rho(\mathbf{q})k' | H_{\rm QPC} | k \rangle = \phi_\rho(|\mathbf{k} - \mathbf{q}/2|)\delta(\mathbf{k}' + \mathbf{q} - \mathbf{k}) \frac{\gamma}{4} \frac{1}{\sqrt{3\pi}} \langle \tfrac{1}{2} m_f | \tau \cdot \hat{\boldsymbol{\phi}}_\rho (\mathbf{V} + i(\boldsymbol{\sigma} \times \mathbf{V}) \cdot \hat{\boldsymbol{\epsilon}}_{M_v}) | \tfrac{1}{2} m_i \rangle . \tag{6.43}$$

One may determine ρ-nucleon coupling constants and form factors by using Eq. (6.40), replacing ω by ρ. All quark models provide essentially identical wave functions for the ω and ρ mesons. The ρ and ω nucleon form factors are then identical, so I examine only sums of vector and tensor coupling constants. I find

$$\frac{g^\rho + f^\rho}{g^\omega + f^\omega} = \frac{5}{3} , \tag{6.44}$$

in reasonable accord with measured values.

F. Delta-nucleon coupling

The form of the pion-quark coupling term of Eqs. (6.15) and (6.17) requires $G_{\pi N\Delta}/G_{\pi NN}$ to have the SU(6) quark model value of $\frac{6}{5}\sqrt{2}$, if the Δ and nucleon wave functions are identical.

The effect of any Δ-N size difference on computed coupling constants can be easily estimated by evaluating integrals like (6.37) and a Gaussian parametrization of the wave functions. The latter approximation should be reasonable at low q. Straightforward evaluation gives

$$\frac{G_{\pi N\Delta}}{G_{\pi NN}} = \frac{6}{5}\sqrt{2} \left[\frac{1 + 8R_\pi^2/9R_N^2}{1 + 8R_\pi^2/9R_\Delta^2} \right]^{3/2} , \tag{6.45}$$

for which the pion, nucleon and delta mean square radii are denoted R_π^2, R_N^2, and R_Δ^2. In Ref. 9 Carlson *et al.* find $R_\pi = 0.29$ fm and $R_N = R_\Delta = .36$ fm. In that case the bracketed factor is unity. Including the effects of the hyperfine interaction on the wave functions[9] leads to $R_\pi = 0.16$ fm, $R_N = 0.32$ fm, and $R_\Delta = 0.39$ fm. Then $G_{\pi N\Delta}/G_{\pi NN}$ is increased by a modest factor of 1.1.

Consider also the ratio $G_{\rho N\Delta}/G_{\rho NN}$. This is the same as in standard quark models if hadronic size differences are ignored. A numerical estimate is given herein.

G. Numerical results

I apply a theory that yields a good description of the meson decays to the computation of the baryon-nucleon coupling constants. There are two recent extensive treatments, one due to Kokoski and Isgur (KI), the other is that of Kumano and Pandharipande (KP). KI and KP adopt different phase space factors that are not the standard relativistic ones, shown in Eq. (6.13). Moreover, there are other differences. In the following I refer only to the $^3P_0$ versions of each. KI employ the meson wave functions of Godfrey and Isgur which include the effects of the gluonic hyperfine interaction and achieve a good description of the energy levels and transition rates. On

the other hand, KP find a satisfactory description of the meson decays by using wave functions in which the hyperfine interaction is ignored (and the mass difference between the ρ meson and pion vanishes). For this reason, the results obtained with the KI treatment are presented first and discussed in more detail. A comparison is made herein.

Start with the pion-nucleon coupling constant. The quantity γ is to be obtained and Eqs. (6.24) and (6.25) are to be evaluated. As noted previously, using the KI modification of these is required in order to maintain consistency with their calculation of meson decay. This is to use the pion mass $\tilde{m}_\pi = 0.72$ GeV instead of $E_\pi(k_1)$ in Eq. (6.13) and to use $\tilde{m}_\pi$ instead of m_π in Eqs. (6.24) and (6.25). Once these kinematic features are established, the necessary numerics are straightforward. The resulting pion-nucleon coupling constant $G_{\pi NN} = 13.2$ which is in remarkable agreement with the experimental value of 13.4. For values of the momentum transfer (q) less than 5 fm^{-1}, the computed form factor $V(q)$, is well parametrized by a dipole form

$$V(q) = 1/[1+(q/\Lambda_\pi)^2]^2 , \tag{6.46}$$

with $\Lambda_\pi = 11.4$ fm^{-1}. This value of Λ_π corresponds to a cloudy bag model[40] form factor

$$[V(q) = 3j_1(qR)/qR]$$

of radius 0.39 fm. This small size, and the consequent "hardness" of $V(q)$ is a consequence of the small intrinsic sizes of the nucleon and pion in the treatments of Refs. 9 and 10. Values of computed coupling constants and form factors are summarized in Table I.

The possibility that the pion cannot be represented by a single $q\bar{q}$ wave function is mentioned previously. One can examine the dependence of the computed value of $G_{\pi NN}$ on the pion root-mean-square (rms) radius to determine the sensitivity to the pion wave function. This is done with the KP observation that the mesonic wave functions of flux-tube models are well represented by hydrogenlike wave functions, Eq. (3.2), as long as the rms radius (R_π) is the same. (The computed value of $G_{\pi NN}$ changes by less than one percent if such a substitution is made.) These hydrogenic wave functions can be employed to display the R_π dependence of $G_{\pi NN}$, Fig. 12(a).

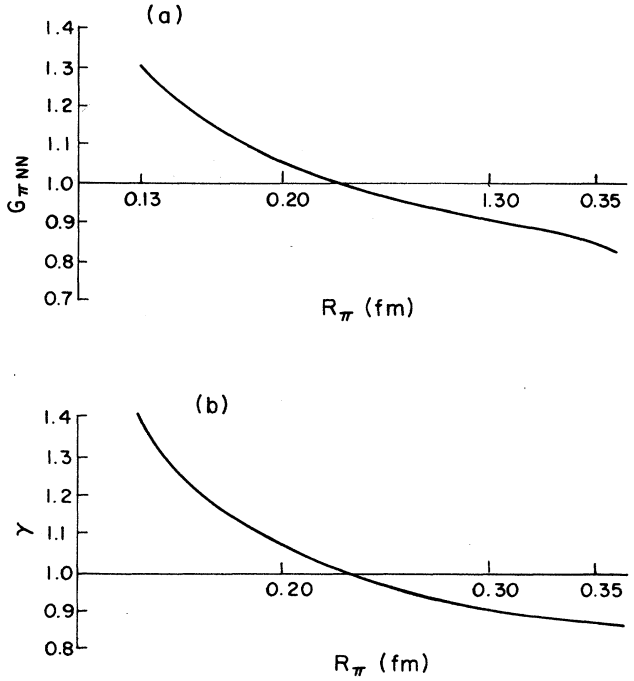

FIG. 12. (a) Dependence of computed value of $G_{\pi NN}$ on R_π, (b) Dependence of computed value of γ on R_π.

There is less than a 40% change in $G_{\pi NN}$ with a variation of R_π by a factor of more than 2.5. This is less dependence than one might expect, and is due to the feature that for each value of R_π the value of γ is readjusted to reproduce the experimental value of $f_{\rho\pi\pi}$. Thus, constraining the computation of $G_{\pi NN}$ to the value of $f_{\rho\pi\pi}$ reduces the sensitivity to the pion wave function.

A final comment about $G_{\pi NN}$ concerns the observation that it is an unrenormalized coupling constant. As a further elaboration, one could apply the cloudy bag model renormalization prescription.[40] That would go beyond the concern of this paper, which is to address qualitative issues.

Next turn to the ω-nucleon coupling. Recalls Eqs. (6.41) and (6.42). Numerical integration yields

TABLE I. Summary of computed coupling constants (meson three momentum is **0**) and vertex functions (dipole parameter Λ).

Quantity	Calculated	Experiment (Ref. 41)
$G_{\pi NN}$	13.2	13.4
$(g^\omega + f^\omega)$	9.9	11–15
$(g^\rho + f^\rho)/(g^\omega + f^\omega)$	1.67	1.7–2.4
$G_{\pi N\Delta}/G_{\pi NN}$	1.87	1.02–1.7
$G_{\rho N\Delta}/G_{\pi N\Delta}$	1.25	quark model and nucleon-nucleon potential model fits to phase shifts
Λ_π	2250 MeV/c	
$\Lambda_{\omega,\rho}$	2250 MeV/c	

$g_\omega + f_\omega = 9.9$. This is 0.75 times $G_{\pi NN}$. This factor, 0.75, can be understood as coming from these sources: the SU(6) nature of the dominant part of the nucleon wave function gives 0.6; a kinematic factor $(m_\omega/\tilde{m}_\pi)^{1/2}$ gives 1.03 and the increased size of the omega meson (the rms radius is 0.32 fm vs 0.194 fm for the pion) of 1.21. The increase associated with an increased meson size arises from an increase in the volume of overlap. The use of harmonic oscillator wave functions would give computed meson-baryon (B) coupling constants a meson radius (R_M) dependence of the form

$$R_M^{3/2}[1+\tfrac{8}{9}(R_M/R_B)^2] .$$

The experimental determinations of the omega-nucleon coupling constant are shown in Table I. Our value 9.9 is in good agreement. It is unfortunate that the nonrelativistic approach employed does not yield a value of f_ω/g_ω. However, the significant feature is that there is a strong omega-nucleon coupling. This is necessary to reproduce the nucleon-nucleon short-distance repulsion.

The computed form factor $V_\omega(q)$ is essentially the same as $V(q)$ except at large values of q. Computed form factors have a weaker dependence on the meson radius than the coupling constant. This can be seen using oscillator parametrizations of the wave functions in the equations of Sec. VI.

Knowledge of the ρ-meson coupling constants is achieved without further computation. The ratio Eq. (6.44) may be compared with the range of experimental values, Table I. The agreement with experiment is quite good.

The $\pi N\Delta$ and $\rho N\Delta$ coupling constants are discussed in Sec. VI F. Numerical results are tabulated in Table I. Qualitative agreement is obtained.

Now turn to the application of the KP theory of meson decays. These authors do not use the $\tilde{m}_\pi$ of KI. Instead they replace the factor E_π of Eq. (6.13) by m_π. As a result, their description of the $\rho \to \pi\pi$ decay requires a larger pion radius and a smaller value of γ, see Fig. 12(b). (The value of γ must be decreased because γ goes as the inverse of the smaller phase space factor.) Thus the KP use of a pion of rms radius 0.32 fm (vs 0.19 fm of KI) gives a good description of the meson decays. They make no kinematic modification to Eqs. (6.24)–(6.25). This would make the KP value of $G_{\pi NN}$ a factor of

$$(\tilde{m}_\pi/m_\pi)^{1/2} = 2.23$$

bigger than that of KI. However, the KP favor a larger pion radius of 0.32 fm which gives a reduction factor of 1.22. (The baryon wave functions of the two approaches are fairly similar, so I used the ones of Capstick and Isgur in all computations.) The net result is the KP coupling constant is 1.82 times that of KI. This difference indicates the sensitivity to different treatments of relativistic effects.

The results are summarized in Table I. SCQCD does yield substantial meson nucleon coupling constants in qualitative agreement with experiment. The numerical agreement with the pion-nucleon coupling constant is impressive, but perhaps accidental. More effort is needed to understand relativistic effects, especially to learn about f_v/g_v.

VII. DISCUSSION

The central features of the meson-baryon dynamics of conventional nuclear physics are that baryons in nuclei obey the Pauli principle (quark-exchange effects of Sec. IV are small), gluonic effects in nucleon-nucleon interactions are very small, and, that meson-baryon coupling constants are large enough to describe nucleon-nucleon scattering. The present manuscript is devoted to examining the question of whether QCD yields these features. The results indicate that the strong coupling version of QCD (SCQCD as defined earlier) does reproduce the underlying dynamical aspects of the conventional treatment.

Many assumptions are required to reach the preceding conclusion. Perhaps the most significant is that SCQCD is valid at all in any regime of momentum transfer. Reaching the stated results required further detailed assumptions. That nucleons in nuclei obey the Pauli principle requires the narrowness of flux tubes and, that the influence of the gluon condensate is estimable in SCQCD. The computation of meson-baryon coupling constants could be improved in several ways. The derivation of the basic string-breaking operator should start with a chirally symmetric fermion Hamiltonian. Perhaps gluonic exchang effects should be included. A more complete treatment of the pion, including a correct calculation of the pion decay constant f_π, would be desirable. The use of relativistic kinematics and dynamics seems to be necessary.

Reducing the number of assumptions will require much effort. However, speaking qualitatively, one can say that SCQCD does reproduce the central meson-baryon dynamics that serve as the theoretical underpinning of the theory of nuclei.

For the moment, I ignore the assumptions and qualifications discussed earlier and briefly examine the implications of this "derivation of nuclei". The lack of significant quark-exchange (QE) effects due to Pauli exchange is an important feature. Any experiment providing definitive evidence for the existence or lack of QE would be very significant. Another implication is that, for ordinary nuclei, wave function components in which the quarks are partially deconfined are essentially absent. For example, the nuclear formation of six quark bags seems to be smaller than previous estimates.[42] The SCQCD derivation of nuclear physics indicates that quark aspects of ordinary nuclei are hidden in the hadronic degrees of freedom. Other consequences are for nucleon-antinucleon annihilation into mesons. In the SCQCD picture such processes proceed via a locally gauge invariant two quark-two antiquark intermediate state.[43]

On the other hand, for large enough values of the momentum transfer, this derivation has no validity. The quarks and gluons need not be confined to hadronic packages. The heavy-ion experiments aimed at observing deconfinement have been discussed heavily. Deconfinement effects should also be observable with high energy leptonic and hadronic probes of nuclei.

ACKNOWLEDGMENTS

I thank S. Godfrey and S. Capstick for providing wave functions. I also thank S. Capstick for explaining his techniques, and H. C. Doenges for useful discussions. E. M. Henley provided useful comments on the manuscript. This work was supported in part by the U.S. Department of Energy. The manuscript was submitted while the author was a visitor at TRIUMF.

[1]J. Kogut and L. Susskind, Phys. Rev. D **11**, 395 (1975).

[2]L. Susskind, in *Coarse Grained Quantum Chromodynamics,* Proceedings of the Les Houches Summer School of Theoretical Physics, edited by R. Balian and C. H. Llewellyn Smith (North-Holland, Amsterdam, 1978); J. B. Kogut, in *Proceedings of the International School of Physics "Enrico Fermi,"* edited by N. Cabibo (North-Holland, Amsterdam, 1987), p. 315.

[3]M. Bander, Phys. Rep. **75**, 206 (1981).

[4]*Gauge Theories of Strong and Electroweak Interactions,* P. Becher, M. Böhm, and J. Joos (Wiley, New York, 1984), Chap. 2.6.

[5]J. Kogut, R. Pearson, and J. Shigemitsu, Phys. Lett. **98B**, 63 (1981).

[6]This point is made in many textbooks. The following are but two examples. M. A. Preston and R. K. Bhaduri, *Structure of the Nucleus* (Addison-Wesley, MA, 1975); A. de Shalit and H. Feshbach, *Theoretical Nuclear Physics* (Wiley, New York, 1974).

[7]G. Krein and Th. A. J. Maris, Phys. Rev. C **36**, 365 (1987).

[8]N. Isgur and J. Paton, Phys. Rev. D **31**, 2910 (1985).

[9]J. Carlson, J. Kogut, and V. R. Pandharipande, Phys. Rev. D **27**, 233 (1983); **28**, 2807 (1983).

[10]S. Godfrey and N. Isgur, Phys. Rev. D **32**, 189 (1985).

[11]S. Capstick and N. Isgur, Phys. Rev. D **34**, 2809 (1986).

[12]G. A. Miller, Phys. Rev. D **37**, 2431 (1988).

[13]R. Kokoski and N. Isgur, Phys. Rev. D **35**, 907 (1987).

[14]S. Kumano and V. R. Pandharipande, Phys. Rev. D **38**, 146 (1988).

[15]A. Hasenfratz and P. Hasenfratz, Annu. Rev. Nucl. Part. Sci. **35**, 601 (1985).

[16]Y. Nambu and G. Jona-Lasinio, Phys. Rev. **122**, 345 (1961); **124**, 246 (1961); see also the review, A. Le Yaouanc *et al.*, in *The Elementary Structure of Matter,* edited by J.-M. Richard, E. Aslanides, and N. Boccara (Springer-Verlag, Berlin, 1988), p. 15.

[17]R. B. Pearson, J. Richardson, J. Shigimetsu, J. B. Kogut, and D. K. Sinclair, Phys. Rev. D **23**, 2945 (1981).

[18]J. B. Kogut and D. B. Sinclair, Phys. Rev. D **24**, 1610 (1981).

[19]J. H. Merlin and J. Paton, Phys. Rev. D **36**, 902 (1987).

[20]M. Lüscher, Nucl. Phys. **B180**, 317 (1981).

[21]R. Sommer, Nucl. Phys. **B291**, 673 (1987); see also the review, C. Michael, University of Liverpool Report LTH-213, 1988.

[22]D. G. Caldi and T. Sterling, Phys. Rev. Lett. **60**, 2454 (1987).

[23]W. Buchmüller, Phys. Lett. **112B**, 479 (1982).

[24]O. W. Greenberg and J. Hietarinta, Phys. Rev. D **22**, 993 (1980).

[25]O. W. Greenberg and J. Hietarinta, Phys. Lett. **86B**, 309 (1979).

[26]P. Hoodbhoy and R. L. Jaffe, Phys. Rev. D **35**, 113 (1987); P. Gonzalez, V. Sanjose, and V. Vento, Phys. Lett. B **1963**, 1 (1987): T. de Forest and P. J. Mulders, Phys. Rev. D **35**, 2849 (1987); P. J. Mulders and A. E. L. Dieperink, Nationaal Instituut voor Kernfysica en Hoge-Energiefysica Report NIKHEF-P-11-1987.

[27]V. F. Weisskopf, Science **113**, 101 (1951); G. C. Gomes *et al.*, Ann. Phys. (N.Y.) **3**, 241 (1958).

[28]D. Robson, Phys. Rev. D **35**, 1029 (1986).

[29]J. B. Kogut *et al.*, Nucl. Phys. **B225**, 326 (1983).

[30]M. A. Shifman *et al.*, Nucl. Phys. **B147**, 385 (1979); **B147**, 447 (1979); **B147**, 519 (1979).

[31]With such a value of g strong coupling holds. Using smaller values would lead to a result of smaller magnitude in (4.20). One can obtain $g(a)$ for large a by using the dg/da of Ref. 5 along with (Ref. 15) $g(a=0.1\text{ fm})\approx 1$.

[32]F. Lenz *et al.*, Ann. Phys. (N.Y.) **170**, 65 (1986).

[33]D. Robson, Phys. Rev. D **35**, 1018 (1987).

[34]Y. Nambu and B. Bambah, Phys. Rev. D **26**, 2871 (1982).

[35]C. J. Horowitz *et al.*, Phys. Rev. D **31**, 1689 (1985).

[36]More detailed treatments of adiabatic surfaces are discussed by N. Isgur, in *Relativistic Dynamics and Quarks in Nuclear Physics,* edited by M. B. Johnson and A. Picklesimer (Wiley, New York, 1986), p. 619. The recent work of A. M. Green and J. Paton [Nucl. Phys. (in press)] confirms the small results found in Ref. 12.

[37]A. Le Yaouanc, *et al.*, Phys. Rev. D **8**, 2223 (1973); **9**, 1415 (1974); **11**, 1272 (1975).

[38]The $^3P_0$ model has been recently applied to the decay of nonstrange baryon resonances by Fl. Stancu and P. Stassart, Phys. Rev. D **38**, 233 (1988); see also S. Kumano, Phys. Lett. B **214**, 132 (1989).

[39]A. Gal, Ann. Phys. (N.Y.) **49**, 341 (1968).

[40]A. W. Thomas, *Advances in Nuclear Physics,* edited by J. W. Negele and E. Vogt (Plenum, New York, 1984), Vol. 13, p. 1; G. A. Miller, in *Quarks and Nuclei, International Review of Nuclear Physics I, 1984,* edited by W. Weise (World-Scientific, Singapore, 1984).

[41]O. Dumbrajs *et al.*, Nucl. Phys. **B216**, 277 (1983). Values of coupling constants determined from nucleon-nucleon scattering are given in R. Machleidt *et al.*, Phys. Rep. **149**, 1 (1987); see also, R. Koch and E. Pietarinen, Nucl. Phys. **A336**, 331 (1980).

[42]G. A. Miller, Phys. Rev. Lett. **53**, 2008 (1984).

[43]A. M. Green and J. A. Niskanen, Mod. Phys. Lett. A **1**, 441 (1986).